(12) INTERNATIONAL APPLICATION PUBLISHED UNDER THE PATENT COOPERATION TREATY (PCT)

(19) World Intellectual Property Organization
International Bureau

(43) International Publication Date
07 June 2018 (07.06.2018)

WIPO | PCT

(10) International Publication Number
WO 2018/102728 A1

(51) International Patent Classification:
A01H 5/00 (2018.01) *C12N 9/90* (2006.01)
C12N 1/13 (2006.01) *C12N 15/09* (2006.01)
C12N 5/10 (2006.01) *C12N 15/82* (2006.01)

(21) International Application Number:
PCT/US2017/064286

(22) International Filing Date:
01 December 2017 (01.12.2017)

(25) Filing Language: English

(26) Publication Language: English

(30) Priority Data:
62/428,775 01 December 2016 (01.12.2016) US

(71) Applicant: **ARKANSAS STATE UNIVERSITY - JONESBORO** [—/US]; P.O. Box 2760, State Univesity, Jonesboro, AR 72467 (US).

(72) Inventors: **LORENCE, Argelia**; 2613 Gallaway Lane, Jonesboro, AR 72404 (US). **YACTAYO-CHANG, Jessica, Patricia**; 114 Drive Street, Jonesboro, AR 72401 (US).

(74) Agent: **ROBINSON, Ross, T.** et al.; Winstead PC, P.O. Box 131851, Dallas, TX 75313 (US).

(81) Designated States *(unless otherwise indicated, for every kind of national protection available)*: AE, AG, AL, AM, AO, AT, AU, AZ, BA, BB, BG, BH, BN, BR, BW, BY, BZ, CA, CH, CL, CN, CO, CR, CU, CZ, DE, DJ, DK, DM, DO, DZ, EC, EE, EG, ES, FI, GB, GD, GE, GH, GM, GT, HN, HR, HU, ID, IL, IN, IR, IS, JO, JP, KE, KG, KH, KN, KP, KR, KW, KZ, LA, LC, LK, LR, LS, LU, LY, MA, MD, ME, MG, MK, MN, MW, MX, MY, MZ, NA, NG, NI, NO, NZ, OM, PA, PE, PG, PH, PL, PT, QA, RO, RS, RU, RW, SA, SC, SD, SE, SG, SK, SL, SM, ST, SV, SY, TH, TJ, TM, TN, TR, TT, TZ, UA, UG, US, UZ, VC, VN, ZA, ZM, ZW.

(84) Designated States *(unless otherwise indicated, for every kind of regional protection available)*: ARIPO (BW, GH, GM, KE, LR, LS, MW, MZ, NA, RW, SD, SL, ST, SZ, TZ, UG, ZM, ZW), Eurasian (AM, AZ, BY, KG, KZ, RU, TJ, TM), European (AL, AT, BE, BG, CH, CY, CZ, DE, DK, EE, ES, FI, FR, GB, GR, HR, HU, IE, IS, IT, LT, LU, LV, MC, MK, MT, NL, NO, PL, PT, RO, RS, SE, SI, SK, SM, TR), OAPI (BF, BJ, CF, CG, CI, CM, GA, GN, GQ, GW, KM, ML, MR, NE, SN, TD, TG).

Published:
— *with international search report (Art. 21(3))*

(54) **Title:** METHOD OF IMPROVING CHLOROPLAST FUNCTION AND INCREASING SEED YIELD

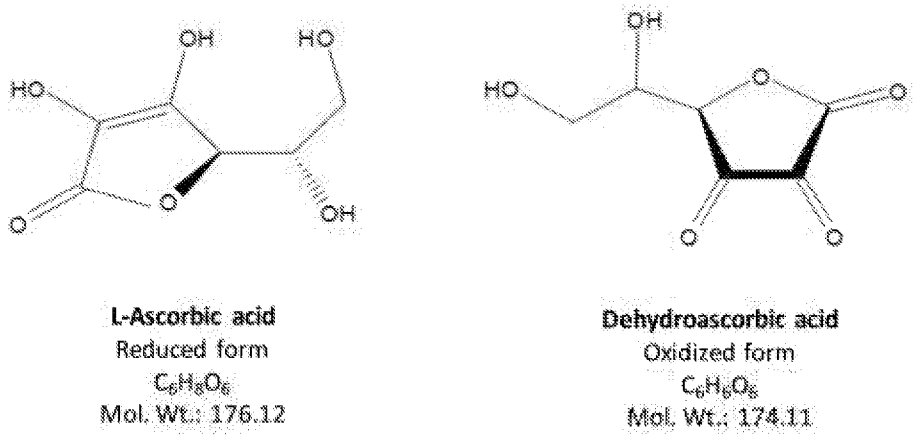


FIG. 1

(57) **Abstract:** Ascorbate protects tissues against damage caused by reactive oxygen species (ROS) produced through normal metabolism or generated from stress. The inositol route to AsA involves four enzymes: *myo*-inositol oxygenase, glucuronate reductase, gluconolactonase (GNL), and L-gulono-1,4-lactone oxidase (GulLO). Eighteen putative GNLs were identified in Arabidopsis, one of which, *AtGNL*, is interesting because it possesses a chloroplastic signal peptide. Knockouts on this gene had lower foliar AsA and stunted growth compared to controls. The functional gene restored the phenotype of the knockouts, and those plants had higher AsA content, enhanced photosynthetic capacity, and higher seed yield.

WO 2018/102728 A1

METHOD OF IMPROVING CHLOROPLAST FUNCTION AND INCREASING SEED YIELD

CROSS-REFERENCE TO RELATED APPLICATIONS

This application claims priority to and is a continuation in part of U.S. Patent Application No. 62/428,775 entitled "Method of Improving Chloroplast Function" filed on December 1, 2016.

STATEMENT REGARDING FEDERALLY SPONSORED RESEARCH OR DEVELOPMENT

Not Applicable.

REFERENCE TO A MICROFICHE APPENDIX

Not Applicable.

RESERVATION OF RIGHTS

A portion of the disclosure of this patent document contains material which is subject to intellectual property rights such as but not limited to copyright, trademark, and/or trade dress protection. The owner has no objection to the facsimile reproduction by anyone of the patent document or the patent disclosure as it appears in the Patent and Trademark Office patent files or records but otherwise reserves all rights whatsoever.

BACKGROUND OF THE INVENTION

1. Field of the Invention

1.1. Vitamin C

Vitamin C (a.k.a. L-ascorbic acid, AsA) is the most abundant water-soluble antioxidant found in plants (Smirnoff, 2000). In the late 1750's it was established that citrus fruits contained a "cure" for scurvy a.k.a. "sea plague". However it was 1928 when Albert Szent-Györyi isolated ascorbate and identified it as the anti-scorbutic component present in citrus and other fruits. Since then, a significant body of evidence has been accumulated about the importance of vitamin C for human and animal health (Drouin *et al.*, 2011; Padayatty, 2016).

Ascorbate is a non-enzymatic antioxidant with a simple molecular structure. As is true for many other antioxidants, vitamin C is present in plants in two forms, the reduced and most active form called ascorbate and the oxidized form named dehydroascorbate. The chemical structure of ascorbate (AsA) and dehydroascorbate (DHA), the reduced and oxidized forms of vitamin C, are shown in FIG. 1. Ascorbate belongs to the family of six carbon sugars with a conjugated pi enediol system at carbons 2 and 3. Ascorbate is a very effective antioxidant due to its ability to donate a pair of electrons and stabilize the subsequent charge using the two oxygen atoms at C2 and C3 in the oxidized form of the molecule (Lee *et al.*, 2006). Ascorbate eliminates reactive oxygen species (ROS) from both inside and outside cells, because it is able to pass through the cell membrane in its oxidized form where it reduces the lipophilic α-tocopherol (vitamin E) which is membrane bound in its oxidized state. This makes ascorbate an important part of the enzymatic antioxidant

cycle in recycling other important antioxidants which would otherwise be lost to the cell (Traber and Stevens, 2011).

1.2. Importance of ascorbate in humans

Humans, primates, and a few other animals including teleost fishes, guinea pigs, some bats and passeriforme birds cannot synthesize vitamin C due to of the lack of an active L-gulono-1,4-lactone oxidase (GuILO) (Drouin *et al.*, 2011). This enzyme catalyzes the last step in vitamin C biosynthesis, and it is highly mutated and non-functional in these species (Sato *et al.*, 1976). Humans and other animals need to consume this essential vitamin from fresh fruits and vegetables to satisfy their needs.

In animals, vitamin C is involved in the synthesis of collagen, an important component of the skin, scar tissue, tendons, ligaments, and blood vessels (Levine *et al.*, 1995; Davey *et al.*, 2000). Another essential role of vitamin C is related to its function in redox homeostasis; this means when the production of ROS increases, the body's response will increase the activity of the endogenous antioxidant system through redox signaling (Figueroa-Méndez and Rivas Arancibia, 2015). Vitamin C functions in oxidative protein folding and in the maintenance of the intraluminal oxidative environment, which suggests that it has a particular role in endoplasmic reticulum related processes (Mandl *et al.*, 2009). In animals, vitamin C interacts enzymatically and non-enzymatically with ROS. In humans vitamin C is essential in preventing pathological conditions including cardiovascular disease, cancer, hepatitis, bacterial infections, fungal infection, and allergies (Cathcart, 1981; Padayatty *et al.*, 2006). The two-time Nobel Prize-winner, Linus Pauling, demonstrated that cancer patients treated with high doses of vitamin C had an increased survival rate (Cameron and Pauling, 1976). Recently Yun *et al.*, (2015) showed that high

levels of vitamin C killed human colorectal cancer cells. This effect is due to increased uptake of dehydroascorbate, the oxidized form of the molecule. Vitamin C has a uricosuric effect in humans and decreases uric acid levels, exerting a protective effect on gout (Stamp *et al.*, 2013).

1.3. Importance of ascorbate in plants

In plants, ascorbate (AsA) has a wide variety of physiological roles. It functions as an enzyme cofactor, as a radical scavenger, and as donor/acceptor of electron transport in the chloroplast (Conklin and Barth, 2004; Ishikawa *et al.*, 2006). Ascorbate can protect tissues against damage caused by ROS produced through normal oxygenic metabolism or generated from biotic and abiotic stress, and is strongly associated with photosynthesis and respiration. Reactive oxygen species include molecules such as superoxide and hydrogen peroxide.

Chloroplasts as well as mitochondria produce ROS as byproducts of normal cellular metabolism, but this production is enhanced by a variety of environmental stresses (Conklin *et al.*, 1996; Conklin and Barth, 2004). Another essential role of AsA is the modulation of processes such as lignification, cell division, cell elongation, the hypersensitive response, tolerance to stresses, and senescence in plants (Smirnoff and Wheeler, 2000; Barth *et al.*, 2004; Pavet *et al.*, 2005). In addition, AsA controls flowering time through phytohormones (Barth *et al.*, 2004). Ascorbate can accumulate at millimolar concentrations in both photosynthetic and non-photosynthetic tissues (Foyer *et al.*, 1983). This accumulation in such high quantities suggests that AsA is important for the plant as a major antioxidant.

1.4. The ascorbate metabolic network

The biosynthetic pathway for vitamin C in animals was elucidated in the early 1950s and was proposed based on *in vivo* radio-labelling and feeding experiments in rats (Ishikawa *et al.*, 2006). There is a single biosynthetic pathway for vitamin C in animals. Evidence obtained during the last 18 years indicates that there are four pathways that lead to the formation of AsA in plants. These routes are the D-mannose/L-galactose (Wheeler *et al.*, 1998), L-gulose (Wolucka and Van Montagu 2003), D-galacturonate (Agius *et al.*, 2003), and *myo*-inositol (Lorence *et al.*, 2004) pathways. FIG. 2 shows this ascorbate metabolic network.

1.4.1. The D-mannose/L-galactose pathway

It is commonly known as the "Smirnoff/Wheeler" pathway. All the genes involved in this route have been characterized. The starting precursor for this route is D-glucose, which is converted to GDP-D-mannose followed by L-galactose that leads to AsA production. D-Glucose-6-P is then converted to GDP-D-mannose by a series of steps catalyzed by fructose-6-P, D-mannose-6-P, and D-mannose-1-P, and that include the *vtc1* mutant locus (GDP-mannose pyrophosphorylase). All of these enzymes have been cloned and characterized (Conklin *et al.*, 1999; Qian *et al.*, 2007; Maruta *et al.*, 2008). The conversion of GDP-D-mannose to AsA comprises four steps: GDP-L-galactose, L-galactose-1-P (Laing *et al.*, 2004), L-galactose (Gatzek *et al.*, 2002) and L-galactono-1,4-lactone (Imai *et al.*, 1998). The GDP-D-mannose to GDP-L-galactose reaction is catalyzed by GDP-D-mannose-3',5'-epimerase a.k.a. GME (Wolucka and Van Montagu, 2003). The vtc2 enzyme and its close homolog *vtc5* convert GDP-L-galactose into L-galactose-1-P

(Smirnoff *et al.*, 2001; Dowdle *et al.*, 2007; Linster *et al.*, 2007). The L-galactose-1-phosphate phosphatase (locus *vtc*4 in Arabidopsis) converts L-galactose-1-P into L-galactose (Conklin *et al.*, 2006). L-Galactose is oxidized at the C1-position by an L-galactose dehydrogenase (GalDH) present in the cytosol to L-galactono-1,4-lactone (Wheeler *et al.*, 1998; Gatzek *et al.*, 2002). All enzymes in this pathway are cytosolic except the last step involving the oxidation of galactono-1-4-lactone to AsA that is carried out by the mitochondrial L-galactono-1,4-lactone dehydrogenase (GLDH), (Østergaard *et al.*, 1997; Imai *et al.*, 1998).

1.4.2. The L-gulose pathway

The L-gulose pathway uses a similar precursor as the D-mannose/L-galactose to the branch point at GDP-D-mannose. GDP-D-mannose is then converted by the GME enzyme into GDP-L-gulose. It is proposed that GDP-L-gulose is converted to L-gulono-1,4-lactone and to AsA in three subsequent steps catalyzed by GDP-L-gulose pyrophosphatase, L-gulose-1-phosphate phosphatase, and L-gulose dehydrogenase respectively (Wolucka and Van Montagu, 2003). The only enzyme that has been characterized in this pathway is GME and it is known to be cytosolic.

1.4.3. The D-galacturonic acid pathway

Observations made in ripening strawberries established that D-galacturonic acid and its methyl ester can be metabolized to form AsA (Mapson and Isherwood, 1956, Loewus and Kelly, 1961). In addition to these early observations the discovery of a D-galacturonic acid reductase (*GalUR*) gene from strawberry (Agius *et al.*, 2003) provide the

main evidence supporting this route. To date GalUR is the only enzyme identified in this route, which has been shown to be cytosolic (Agius *et al.*, 2003).

1.4.4. The *myo*-inositol pathway

Biochemical and molecular data indicate that *myo*-inositol can also be a precursor for the biosynthesis of AsA in Arabidopsis (Lorence *et al.*, 2004). This pathway involves four enzymes, starting from the oxidation of *myo*-inositol to D-glucuronic acid and further reduction to L-gulonic acid and to L-gulono-1,4-lactone, and further oxidation to AsA. These conversions are catalyzed by *myo*-inositol oxygenase (MIOX), glucuronate reductase (GlcUR), gluconolactonase (GNL), and L-gulono-1,4-lactone oxidase (GulLO) respectively. The first two enzymes have already characterized by the Lorence Laboratory. *Arabidopsis thaliana* lines over-expressing MIOX and GulLO are tolerant to multiple abiotic stresses such as salt, cold, heat, and pyrene (Lisko *et al.*, 2013). These high expressing AsA plants exhibit increased growth and biomass accumulation (Lorence *et al.*, 2004; Lorence and Nessler, 2007; Lisko *et al.*, 2013).

Transgenic rice overexpressing MIOX showed improved growth performance when grown in the presence of 200 mM mannitol and presented higher survival rates compared to wild type plants treated with polyethylene glycol (Duan *et al.*, 2012). MIOX proteins are present in almost all multicellular eukaryotes and are highly conserved across phyla. It has been reported that the role of MIOX and D-GlcUA for AsA biosynthesis in plants is a major plant antioxidant to counterbalance oxidative damage (Shao *et al.*, 2008). The first two enzymes in the inositol pathway to AsA are cytosolic. The Lorence laboratory

has evidence indicating that some isoforms of the last two enzymes in this pathway reside in the chloroplast and the endoplasmic reticulum (ER).

1.5. Role of ascorbate in the chloroplast

Chloroplasts are the organelles responsible for photosynthesis, a process that is essential for plant growth and development (Rustchow *et al.*, 2008; Venkatasalam, 2012). Key metabolites in the photosynthetic process are NADPH and ATP. Although photosynthesis is an essential process, light absorption creates oxidative stress due to the formation ROS, such as singlet oxygen ($^1O_2$), superoxide (O_2^-) and hydrogen peroxide (H_2O_2) (Oelze *et al.*, 2008). Under high light, the electron flow through the photosynthetic chain overcomes the passage of electrons from ferredoxin to several reductases, and this causes an over-reduction of the plastoquinone and cytochrome b complex. Thus, during a day with high irradiance, plants are under constant oxidative stress (Oelze *et al.*, 2008). Light/dark cycles are probably the most important signals that regulate plant development. Light is essential for photosynthesis, but an excess inside the chloroplast leads to excessive ROS. Among the chief defense mechanisms that allow plants to cope with environmental stress situations is the ascorbate-glutathione cycle, a complex metabolic pathway in which a variety of photochemical and enzymatic steps are involved. Ascorbate is essential to detoxify H_2O_2 produced during the Mehler reaction, which is formed by dismutation of O_2^- and can be regenerated via the AsA-glutathione cycle to counteract O_2^- (Halliwell and Foyer, 1976; Foyer and Noctor, 2000; Munné-Bosch and Alegre, 2002; Talla *et al.*, 2011). FIG. 3 shows the Anti-oxidation of reactive oxygen species. Reactive oxygen is generated when electrons (e-) not utilized in photosynthesis are donated to oxygen, thus creating

superoxide (O2.-) that can be converted to hydrogen peroxide (H2O2) by superoxide dismutase (SOD). The H2O2 is further converted to H2O by ascorbate peroxidase (APX) utilizing ascorbate (AsA) as an electron donor that, in turn, becomes oxidized ascorbate (ox-AsA). Additional electrons are consumed via the conversion of ox-AsA back to AsA or the conversion of double ox-AsA back to AsA using glutathione. The resulting oxidized glutathione is reduced by electrons from electron transport by means of glutathione reductase (GR). Source: Demmig-Adams et al., 2012. The demand for AsA in these reactions increases at higher light intensities, when formation of ROS is enhanced. Experimental evidence suggests the existence of an effective signaling network between the chloroplast and the mitochondria that involves ROS and antioxidants (Foyer and Noctor, 2003; Noctor *et al.*, 2007). The different light/dark conditions are currently one of the major challenges in plant research to improve crop productivity under a changing global climate.

Ascorbate is present in all plants although its concentration varies greatly and has been identified in various compartments of the cell. Ascorbate occurs inside as well as outside the chloroplast (Constable, 1963; Hall and Rao, 1999, Habermann, 2013), where it has been shown to accumulate at concentrations up to 50 mM (Hall and Rao, 1999); this represents about 25-30% of the total AsA in the plant cell (Horemans *et al.*, 2000). All known AsA biosynthetic enzymes reside in compartments other than the chloroplast, and therefore it is currently unknown how this organelle is able to accumulate such high concentrations of this antioxidant.

Ascorbate was at one time considered to be a necessary component of the photosynthetic phosphorylation system (Arnon, 1959) however is now considered

important in providing a protective role in preventing inactivation of essential components of the chloroplasts (Pintó-Marijuan and Munné-Bosch, 2014).

It has been recognized for more than a century that chloroplasts alter their distribution within cells depending on the external light conditions. Chloroplasts can be observed to move to positions that maximize photon absorption under low-influence light and, conversely, to move to positions that minimize photon absorption under high light. The movement away from areas of strong light is believed to offer areas of strong light protection against photo-oxidative damage (Eckardt, 2003).

Arabidopsis plants growing under long day conditions (12 h of photoperiod) accelerate flowering in comparison with plants growing under shorter photoperiods. Short days distinctly extend the vegetative phase of Arabidopsis growth and delay senescence (Lepistö and Rintamäki, 2012). In the course of high-light acclimation, elevated ROS production is compensated for by induction of antioxidant systems in leaves which in turn prevent the oxidation of leaf cells (Mittler *et al.*, 2004).

1.6. Definition of the problem

Significant progress has been made in the characterization of *myo*-inositol oxygenase (MIOX) and glucuronate reductase (GlcUR), the first two enzymes of the *myo*-inositol pathway to AsA (Lorence *et al.*, 2004; Lorence and Nessler, 2007). High AsA lines over-expressing MIOX4 and GuILO are tolerant to multiple causes of oxidative stress including salt, cold, heat, and pollutants (Lisko *et al.*, 2013). The third enzyme, GNL, has been characterized in rat, *Zymomonas mobilis*, and *Pseudomonas aeruginosa* (Tarighi *et al.*, 2008), but not in plants. Current research in the Lorence Group focuses on the

characterization of this third enzyme. Preliminary data indicate the presence of isoforms of glucuronolactonase (GNL) that are targeted to the ER and the chloroplasts. This project focuses on gaining insights about the function of a putative GNL that possesses a chloroplastic signal peptide. This is quite relevant as it is currently unknown how this organelle that makes photosynthesis possible, is able to accumulate up to 50 mM AsA.

1.7. Hypothesis and aims for the role of ascorbate in the chloroplast

If *At*1g56500 encodes a functional glucuronolactonase (GNL) that resides in the chloroplast, then this protein will protect this organelle and green tissues, and will counteract reactive oxygen species formed under light stress. When over-expressed in plants this enzyme will confer plants enhanced photosynthetic efficiency.

This hypothesis will be tested by addressing the following aims:

Aim 1: Characterize the *At*GNL (*At*1g56500) functional enzyme.

Aim 2: Establish the role of the *At*GNL under low, normal, and high light conditions.

Aim 3: Characterize the phenotype and photosynthetic efficiency of Arabidopsis lines with low, normal, and high *At*GNL expression.

II. Description of the Known Art

Patents, patent applications, and references disclosing relevant information are disclosed below. These patents, patent applications, and references are hereby expressly incorporated by reference in their entirety.

SUMMARY OF THE INVENTION

Chloroplasts, the organelles responsible for photosynthesis, are essential for plant growth and development, and are involved in the metabolism of carbon, nitrogen, and sulfur (Venkatasalam, 2012; Rustchow *et al.*, 2008). In addition, chloroplasts synthesize amino acids, fatty acids, purine, and pyrimidine bases, isoprenoids, tetrapyrroles, and the lipid components of their own membranes, followed by processing, folding, and assembly by various chaperone systems (Peltier *et al.*, 2006). The chloroplasts need considerable protein import from the cytosol. Chloroplasts control nuclear gene expression indirectly by metabolites, ROS and other cellular processes (Pogson *et al.*, 2008; Pfannschmidtm, 2010).

It has been recognized for more than a century that chloroplasts alter their distribution within cells depending on the external light conditions. Chloroplasts can be observed to move to positions that maximize photon absorption under low light and, conversely, to move to positions that minimize photon absorption under high light. The movement away from areas of strong light is believed to offer protection against photo-oxidative damage (Eckardt, 2003). The photoreceptors responsible for light induced chloroplast movement in higher plants are phototropins. The phototropins PHOT1 and PHOT2 are involved in blue light mediated chloroplast relocation, stomatal opening and phototropism (Briggs and Christie, 2002). PHOT1 is the primary photoreceptor that controls phototropism in low light (Huala *et al.*, 1997), whereas PHOT2 is responsible for the light-avoidance relocation of chloroplast under high light (Kagawa *et al.*, 2001).

Ascorbate (AsA) is found in all plants although its concentrations vary greatly. Within the leaf, ascorbate occurs inside as well as outside the chloroplasts (Constable, 1963; Habermann, 2013). Ascorbate was at one time considered to be a necessary

component of the photosynthetic phosphorylation system but recently it has been regarded as having a protective role in preventing inactivation of essential components of the chloroplasts (Arnon, 1959; Pintó-Marijuan and Munné-Bosch, 2014). Ascorbate helps detoxify H_2O_2 produced during the Mehler reaction, (Foyer and Noctor 2000; Talla *et al.*, 2011) and is important for photoprotection (Demmig-Adams *et al.*, 2012). In chloroplasts, high ascorbate levels are required to overcome photoinhibition caused by strong light (Miyaji *et al.*, 2014).

The *myo*-inositol pathway is one of the four routes for the production of AsA in plants. This pathway has not been completely elucidated. Three enzymes have been characterized: *myo*-inositol oxygenase (MIOX), glucuronate reductase (GlcUR), and L-gulono-1,4-lactose oxidase (GuILO) (Lorence *et al.*, 2004; Lorence and Nessler, 2007, Lisko *et al.*, 2013; Aboobucker, 2014). The third enzyme, gluconolactonase (GNL), has been characterized in *Rattus norvegicus* (Kondo *et al.*, 2006), *Euglena gracilis* (Ishikawa *et al.*, 2008), *Pseudomonas aeruginosa* (Tarighi *et al.*, 2008), *Xanthomonas campestri* (Chen *et al.*, 2008), *Homo sapiens* (Aizawa *et al.*, 2013), and *Gluconobacter oxydans* (Shinagawa *et al.*, 2009), but not in plants.

The first two enzymes in this pathway (MIOX4 and GlcUR) are cytosolic, the fourth enzyme (GuILO) resides in the ER as illustrated in FIG. 4. FIG. 4 shows the Subcellular localization of enzymes in the ascorbate metabolic network. GLDH, the terminal enzyme in the D-mannose/L-galactose pathway is located in the mitochondria, while the terminal enzyme in the *myo*-inositol and L-gulose routes (GulLO) is known to reside in the endoplasmic reticulum. All other enzymes are supposed to be cytoplasmic. However, the localization of the third enzyme (GNL) is unknown. In 2004 gene sequences of well

characterized GNLs from rat and bacteria were aligned and compared to the *Arabidopsis* genome (A. Lorence, personal communication). This resulted in the identification of 18 putative *GNL* candidate genes. FIG. 5 shows the Putative glucuronolactonases (GNLs) in Arabidopsis. The T-DNA knockouts were screened looking for low AsA lines to identify true GNLs in Arabidopsis. The foliar AsA content in knockout lines corresponding to the GNL *Arabidopsis* genes were measured to identify low AsA mutants. Bioinformatics analysis of the genes found that one of the SALK lines with low AsA encodes a protein that possesses a chloroplastic signal peptide. In addition, microarray data available at Genevestigator (Zimmermann *et al.*, 2004) showed that there is a suppression of the expression of this gene (*At1g56500*) when plants are exposed to dark conditions. To understand the role of *At*GNL in plant physiology, two knockout lines with a T-DNA inserted into the *At1g56500* gene were obtained from the Arabidopsis Biological Resource Center (ABRC). FIG. 6 shows the Schematic of the insertion site of the T-DNA in the *At1g565400* gene in SALK lines 026172 and 011623 (red squares). Exons are shown as blue boxes. Source: TAIR database.

The *At1g56500* cDNA was amplified and sub-cloned into the pBIB-Kan vector under the control of the cauliflower mosaic virus 35S promoter and the tobacco etch virus (TEV) enhancer. A 6X-HIS tag was added at the 5' end of the cDNA to facilitate protein detection by Western blot and purification by nickel affinity chromatography.

To confirm that indeed this gene encodes a protein residing in the chloroplast, the *Nicotiana benthamiana* was infiltrated with an *At*GNL construct using an optimized *Agrobacterium*-mediated transient transformation method (Medrano *et al.*, 2009). Chloroplasts were isolated from leaves using a chloroplast isolation kit (CP-ISO Sigma).

A Western blot developed with an anti-HIS antibody, confirmed that *At*GNL is indeed in the chloroplast as illustrated in FIG. 7. FIG. 7 shows the The *At*GNL protein resides in the chloroplast. Chloroplasts were isolated from leaves of *Nicotiana benthamiana* plants infiltrated with the *At*GNL construct using a chloroplast isolation kit (CP-ISO, Sigma). Western blot was done using an anti-HIS antibody. M: molecular weight marker, lane 1 empty vector fraction, lane 2 non chloroplastic fraction, lane 3 chloroplastic fraction, lane 4 chloroplast fraction after purification by nickel affinity chromatography.

This work focuses on characterizing a functional *At*1g56500 (*At*GNL). In this work three aims are proposed: Aim 1: Characterize the *At*GNL (*At*1g56500) functional enzyme, Aim 2: Establish the role of the *At*GNL under low, normal, and high light conditions, and Aim 3: Characterize the phenotype and photosynthetic efficiency of Arabidopsis lines with low, normal, and high *At*GNL expression.

Vitamin C (L-ascorbic acid, AsA) is the most abundant water-soluble antioxidant in plants. Ascorbate scavenges free radicals, is an enzyme cofactor, and a donor/ acceptor of electrons in the chloroplast. Ascorbate protects tissues against damage caused by reactive oxygen species (ROS) produced through normal metabolism or generated from stress. The inositol route to AsA involves four enzymes: *myo*-inositol oxygenase, glucuronate reductase, gluconolactonase (GNL), and L-gulono-1,4-lactone oxidase (GulLO). The third enzyme, GNL, has been characterized in rat and bacteria but not in plants. Eighteen putative GNLs were identified in Arabidopsis, one of which, *AtGNL*, is interesting because it possesses a chloroplastic signal peptide. Chloroplasts can accumulate up to 50 mM AsA but until now no chloroplastic AsA biosynthetic genes have been described. This study includes the characterization of the first plant GNL enzyme *in vitro*

and *in planta*. Knockouts on this gene had lower foliar AsA and stunted growth compared to controls. The functional gene restored the phenotype of the knockouts, and those plants had higher AsA content, and enhanced photosynthetic capacity. These results highlight the importance of *At*GNL in AsA formation and in maintaining a healthy redox balance in the leaves particularly under low light stress. *At*GNL is the first AsA biosynthetic enzyme that resides in chloroplasts.

Accordingly, it is an object of the present invention to characterize the *At*GNL (At1g56500) functional enzyme.

It is another object of the present invention to establish the role of the *At*GNL under low, normal, and high light conditions.

It is another object of the present invention to characterize the phenotype and photosynthetic efficiency of Arabidopsis lines with low, normal, and high *At*GNL expression.

It is another object of the present invention to increase photosynthetic efficiency.

It is another object of the present invention to increase *AtGNL* expression.

It is another object of the present invention to provide a method for a purification protocol for *At*GNL recombinant protein.

It is another object of the present invention to increase the levels of AsA within a plant.

It is another object of the present invention to increase the biomass of the plants.

It is another object of the present invention to delay aging of the plants.

It is another object of the present invention to increase production of ATP.

These and other objects and advantages of the present invention, along with features of novelty appurtenant thereto, will appear or become apparent in the course of the following descriptive sections and the attached drawings.

BRIEF DESCRIPTION OF THE DRAWINGS

In the following drawings, which form a part of the specification and which are to be construed in conjunction therewith, and in which like reference numerals have been employed throughout wherever possible to indicate like parts in the various views:

FIG. 1 is a chemical structure view of one embodiment of the present invention;

FIG. 2 is a metabolic network view thereof;

FIG. 3 is a flowchart view thereof;

FIG. 4 is a metabolic network view thereof;

FIG. 5 is a table view thereof;

FIG. 6 is a schematic view thereof;

FIG. 7 is a blot view thereof;

FIG. 8 is a construct view thereof;

FIG. 9 is a table view thereof;

FIG. 10 is a blot view thereof;

FIG. 11 is a blot view thereof;

FIG. 12 is an analytical view thereof;

FIG. 13 is a table view thereof;

FIG. 14 is a graph view thereof;

FIG. 15 is a graph view thereof;

FIG. 16 is a graph view thereof;

FIG. 17 is a table view thereof;

FIG. 18 is a graph view thereof;

FIG. 19 is a photographic and chart view thereof;

FIG. 20 is a photographic view thereof;

FIG. 21 is a chart view thereof;

FIG. 22 is a table view thereof;

FIG. 23 is a chart view thereof;

FIG. 24 is a chart view thereof;

FIG. 25 is a metabolic network view thereof;

FIG. 26 is a chart view thereof;

FIG. 27 is a table view thereof;

FIG. 28 is a chart view thereof;

FIG. 29 is a table view thereof;

FIG. 30 is a chart view thereof;

FIG. 31 is a table view thereof;

FIG. 32 is a photographic view thereof;

FIG. 33 is a phylogenetic view thereof;

FIGS. 34A and 34B are table views thereof;

FIG. 35 is a chart view of one embodiment of the present invention;

FIG. 36 is a genetic sequencing view of one embodiment of the present invention; and

FIG. 37 is a genetic sequencing view of one embodiment of the present invention.

DETAILED DESCRIPTION

Arabidopsis thaliana ecotype Columbia wild type seeds (Col-0, stock # CS60000), SALK_026172, and SALK_011623 were obtained from the Arabidopsis Biological Resource Center (ABRC, Columbus, OH). Seeds were sterilized with 70% (v/v) ethanol for 10 min followed by 50% (v/v) sodium hypochlorite containing 0.05% (v/v) Tween-20 for 15 min. Next, seeds were washed 6 times with sterile water. Finally, seeds were transferred to a petri dish containing medium which consisted of Murashige-Skoog (MS) salts (Murashige and Skoog, 1962), MS vitamins, and 3% (w/v) sucrose, at pH 5.6. The medium was supplemented with 0.04% (w/v) $MgSO_4.7H_2O$. The seeds were vernalized for 3 days at 4°C. Plates were transferred to a growth chamber and incubated at 23°C, 65% humidity, 16:8 h photoperiod and 200 $\mu mol/m^2/s$ light intensity. After establishment, seedlings were transferred to PM-15-13 AIS MIX Arabidopsis soil (Lehle-Seeds, Round Rock, TX) in 2 inch pots. Pots were covered with a dome for one week and after that plants were grown until they reached maturity.

Nicotiana benthamiana seeds were obtained from The Department of Plant Pathology, Physiology and Weed Science at Virginia Polytechnic Institute and State University (Blacksburg, VA). Seeds were sown in 4.5 inch pots containing Pro-mix BX soil (Premier Horticulture Ltd, Canada) with fertilizer Osmocote 14-14-14 (Scotts, Canada). Vermiculite was overlaid on top of the seeds. The pots were covered with a dome for one week. Plants were grown in an environmental control chamber with the following conditions: 25°C (day)/ 21°C (night) temperature, 65% relative humidity, 16:8 h photoperiod, and 150 $\mu mol/m^2/s$ light intensity.

2.2.2. Constructs of interest

Two gene constructs were made for this project. The first construct is one where the cDNA encoding a putative *At*GNL was placed under the control of the 35S promoter and the tobacco etch virus (TEV) enhancer (*At*GNL-6XHIS:pBIB-Kan), (Becker, 1990). In this construct a histidine tag was added to the C-terminus of the protein of interest to allow detection using antibodies and to facilitate purification. The second construct is one where the putative promoter region of the *AtGNL* (a 1000 bp fragment preceding the ATG) was cloned and fused to the *GUS* reporter gene to better understand the spatial and temporal expression of this gene (p*At*GNL:pCAMBIA1305.1). FIG. 8 shows the Constructs of interest. (**A**) The *At*1g56500-HIS:pBIB-Kan construct containing *At*1g56500 (*At*GNL) with a six histidine (6X-HIS) tag and adjacent neomycin phosphotransferase II (*npt*II) selectable marker. (**B**) The pAt1g56500:pCAMBIA1305.1 construct containing the *At*GNL promoter with the *GUS-PLUS* reporter gene and the hygromycin phosphotransferase (*hph*) selectable marker. NOS-P: promoter of nopaline synthase gene, 35S-T: terminator of the 35S cauliflower mosaic virus gene; TEV: tobacco etch virus translational enhancer; LB and RB: left and right T-DNA borders, respectively.

2.2.3. Development of transgenic lines

To study the expression of *At*GNL in *Arabidopsis thaliana*, stable transgenic plants were developed by the floral dip method (Clough and Bent, 1998). Wild type CS60000 and knockouts: SALK_026172 and SALK_011623, were transformed with the *Agrobacterium tumefaciens* GV3101 strain carrying the construct of interest. The T0 seeds were planted on MS medium plus kanamycin. The antibiotic resistant seedlings were transferred to soil

and grown to maturity under the above stated conditions. The presence of the transgene of interest was established via PCR using gene specific primers, and genomic cDNA as a template. To develop homozygous versions of the knockout lines, over-expresser (wild type plus *At*GNL), and restored lines (knockouts plus *At*GNL) T1 plants that were high AsA expressers were identified. The seeds of those plants were sterilized with 70% (v/v) ethanol for 10 min followed by 50% (v/v) sodium hypochlorite containing 0.05% (v/v) Tween-20 for 15 min. Next, seeds were washed 6 times with sterile water. Finally, seeds were transferred to petri dishes containing Murashige and Skoog (MS) medium which consists of salts, MS vitamins, and 3% (w/v) sucrose at pH 5.6. The medium was supplemented with 0.04% (w/v) $MgSO_4.7H_2O$, and 50 mg/L kanamycin. Plated seeds were vernalized for 3 days at 4°C. After establishment, seedlings were transferred to soil and grown under the above stated conditions until they reached maturity. This process was repeated until plants with a 100% germination score in the presence of antibiotic selection were developed.

2.2.4. Ascorbate measurements

In Arabidopsis, *in planta* AsA concentration changes throughout the day as well as during development (Tamaoki *et al.*, 2003; Zhang *et al.*, 2009). Fifty mg of leaf tissue were collected between 9:00 am and 11:00 am. Tissue was frozen immediately in liquid nitrogen and stored at -80°C until analyzed. Reduced, oxidized, and total AsA were measured using a 96-well plate format as described by Haroldsen *et al.*, (2011). Briefly, frozen tissue was pulverized in 6% (w/v) *meta*-phosphoric acid, and centrifuged at 13,000 rpm for 15 min. Reduced AsA was determined by measuring the decrease in absorbance at 265 nm after

addition of 0.5 unit of ascorbate oxidase to 300 µL of the reaction medium containing the plant extract and 100 mM phosphate buffer at pH 6.9. Oxidized ascorbate was measured in a 300 µL reaction mixture with 10 µL of 40 mM dithiothreitol (DTT) after incubation in the dark for 20 min at room temperature. The reaction was followed by measuring absorption at 265 nm. Calculations were made based on a standard curve made with pure L-ascorbic acid run in parallel. Ten biological replicates were measured in analytical triplicate and reported as µmol per gram fresh weight (µmol/ g FW).

2.2.5. Transient expression of *At*GNL in *Nicotiana benthamiana*

In order to test its function the putative GNL recombinant protein was produced in *Nicotiana benthamiana*. This plant is a widely used platform for the production of active proteins, including antibodies, enzymes and other proteins that require post-translational modifications (Klimyuk *et al.*, 2012; Leuzinger *et al.*, 2013). To find the optimal expression time, five week old *N. benthamiana* plants were vacuum infiltrated with the *At1g56500-6XHIS:pBIB-kan* construct as described by Medrano *et al.*, 2009. Leaf tissue was harvested at 24, 48, 72, and 96 h post infiltration for further analysis. The optimum time for tissue collection based on Western blot data, was found to be at 48 h post infiltration (data not shown). In subsequent experiments all leaves were collected at 48 h post-infiltration, frozen immediately in liquid nitrogen and stored at -80°C until further processing. Plants infiltrated with the empty pBIB-kan binary vector (EV) were used as controls for these experiments.

In order to confirm the expression of the *At*GNL in *N. benthamiana*, Western blot experiments were carried out. Crude extracts were made by grinding frozen tissue in the

presence of two volumes of SDS buffer containing 150 mM Tris-HCl pH 6.8, 5 mM EDTA pH 8.0, 30% (v/v) glycerol, 6% (w/v) SDS. The homogenate extract was then centrifuged at 13,000 x g for 15 min, and the supernatant was recovered. Proteins were separated via SDS-PAGE. Six µL of plant extract were mixed with 2.5 µL of SDS loading buffer (4X) and 1 µL of DTT, incubated for 10 min at 70°C and separated by SDS-PAGE on 10% precast mini-gels (Expedeon, San Diego, CA) with a Tris-MOPS buffer. Subsequently, separated proteins were electro blotted onto a nitrocellulose membrane, using transblotting buffer containing: 25 mM Tris base, 192 mM glycine, and 20% methanol. Recombinant *At*GNL-6XHIS was detected using an anti-HIS (C-term)/AP antibody at a 1:2,000 v/v dilution (Invitrogen, Carlsbad, CA) and CDP-start, a chemiluminescent substrate for alkaline phosphatase detection (Roche Diagnostics, Indianapolis, IN).

2.2.6. Recombinant *At*GNL purification

Recombinant *At*GNL protein was purified from *N. benthamiana* leaves. Five grams of leaf tissue were pulverized in liquid nitrogen and proteins were extracted with 10 mL of buffer A (75 mM sodium phosphate dibasic, 25 mM sodium phosphate monobasic, 150 mM NaCl, 10 mM sodium metabisulfite, and 0.6% (v/v) protease inhibitor cocktail, pH 7.4). The extract was then centrifuged at 13,000 x g for 15 min. The supernatant obtained after centrifugation was loaded onto a nickel affinity column (HIS60 Ni Superflow) and incubated for 1 h at 4°C. Then, the column was washed with 50 mM sodium phosphate pH 7.4, 300 mM NaCl, 40 mM imidazole buffer and the bound proteins were eluted with 250 mM of imidazole. The eluate from the nickel column was concentrated using an AMICON® 30K ultra centrifugal filter (Millipore, Billerica, MA). Total soluble protein

concentration was estimated by the Bradford method (Bradford, 1976) using Coomassie blue G-250 dye (Thermo Scientific) and bovine serum albumin (Pierce, Rockford, IL) as a standard. Protein fractions from the purification procedure were separated by SDS-PAGE and the *At*GNL was detected by Western blot and silver staining using Pierce® Silver Stain Kit (Thermo Scientific).

2.2.7. Recombinant *At*GNL enzyme assay

The lactonase activity was assayed *in vitro* based on the decrease in absorbance (405 nm) of the *p*-nitrophenol pH indicator that resulted from the enzymatic opening of the lactone ring when D-glucono-δ-lactone was used as substrate in the presence of the *At*GNL as previously described (Ishikawa *et al.*, 2008). Enzyme preparations were made fresh for individual experiments at room temperature.

In order to establish the optimal enzyme activity for *At*GNL, several conditions were tested. The optimum concentration for enzyme activity was 30 µg per reaction. One mL of the reaction typically contained: 10 mM PIPES pH 6.5, 5 mM D-glucono-δ-lactone, 75 µM $MnCl_2$, 2.5 mM *p*-nitrophenol, and an aliquot of the purified enzyme. An equal amount of boiled enzyme was used as control for these experiments.

In order to examine the specificity of the *At*GNL enzyme for D-glucono-δ-lactone, multiple substrates were tested in the lactonase assay. The substrates used in this experiment were: D-glucono-δ-lactone (D-GuIL), L-galactono-ɤ-lactone (L-GaIL), L-galactonic acid (L-GalA), L-gulono-ɤ-lactone (L-GulL), and L-gulonic acid (L-GulA). The L-GaIA and L-GuIA were prepared by the hydrolysis of L-GaIL and L-GuIL, respectively. For hydrolysis 20 mL of 0.3 M NaOH were added to 100 µL of 10 mM L-GaIL or L-GuIL,

the mixture was vigorously agitated by vortexing for 20 s, and 20 µL of 0.3 M HCl were added to neutralize the solution (Ishikawa *et al.*, 2008). For enzyme kinetic experiments, individual reactions were monitored for 15 min at different substrate concentrations. Analysis was done using the GraphPadPrism 6.2 software.

2.2.8. High throughput phenotyping

To characterize the phenotype of the over-expresser (L60, L61, L62), knockout lines (SALK_026172 and SALK_011623), and restored lines (L89, L90, L100, L128, L129, L130), under low, normal, and high light conditions a high throughput phenotyping platform (Scanalyzer HTS instrument, Lemnatec, Germany) and the LemnaControl software were used. This instrument is equipped with a robotic arm that holds visible (VIS, a.k.a. RGB), fluorescence (FLUO), and near infrared (NIR) high-resolution cameras. This system empowers unbiased, non-invasive, automated, and effective characterization of plant phenotypes. The cameras in the system are as follows: VIS camera, piA2400-17gc CCD (Basler, Ahrensburg, Germany) with resolution of 2454 x 2056 pixels; FLUO camera, scA1600-14gc CCD (Basler, Ahrensburg, Germany) with resolution 1624 x 1234 pixels; and NIR camera, Goldeye GIGE P-008 SWIR (Allied Vision Technologies, Stadtroda, Germany) with resolution 320 x 256 pixels and with spectral sensitivity between 900 and 1700 nm.

In the greenhouse plants were grown in PM-15-13 AIS MIX soil (Lehle-Seeds, Round Rock, TX) in Quickpot 15 trays in a greenhouse during March 12-30 2015 in Jonesboro, AR, USA (latitude 29.4889 and longitude -98.3987). Growth conditions were as follows: 22°C-26°C temperature, 16:8 h photoperiod, 55% humidity and three different

light conditions: low (35-110 μmol/m^2/s), medium (110-350 μmol/m^2/s) and high light (350-700 μmol/m^2/s). Light intensity was recorded four times per day (9:00 am, 12:00 pm, 3:00 pm, and 6:00 pm) to cover the entire sunlight period.

Images of *At*GNL lines were captured every two days between 16 days and 26 days after germination, to cover the full vegetative growth. Images (5670 images = 7 lines x 15 biological replicates x 3 light treatment x 6 times points x 3 cameras) were analyzed using the LemnaGrid Software. The analysis of the RGB images was done as previously described by Arvidsson *et al.*, (2011). Multiple phenotypic parameters were calculated for each plant including: projected leaf area (cm^2), convex hull area (cm^2), caliper length (a.k.a. rosette diameter, mm) and compactness (measure of the bushiness of the plant). From the RGB images the relative area of the plants displaying normal green color versus the area with detectable yellow color (chlorosis) were calculated. The analysis of the NIR images was similar to the color classification of VIS camera, using the acquired gray-scale images, where high water content corresponds to darker tones while low water corresponds to lighter gray tones. The software used this information to calculate the relative area with low, medium, and high water content. The fluorescence camera acquires red-scale images and in this case the red tones were divided into four equidistant bins, and the software calculated the relative area with zero, low, medium, and high fluorescence. Quantitative data obtained from the images were analyzed.

2.2.9. Photosynthetic efficiency

In order to determine photosynthetic efficiency of photosystem II (Φ/II), linear electron flow (LEF), and non-photochemical quenching (NPQt) of the knockout lines

(SALK_026172 and SALK_011623), over-expresser (L61), restored lines (L100 and L129), empty vector, and wild type controls growing under low and normal light conditions were analyzed using a MultispeQ. This is a hand held fluorometer developed by the Kramer Laboratory at Michigan State University. Ten biological replicates were chosen randomly at the same time of day for measurements. Data were visualized in an Android tablet (Samsung Galaxy Tab 4) and analyzed in the PhotosynQ website (www.photosynq.org).

2.2.10. Promoter*At*GNL:GUS expression in *Arabidopsis thaliana*

To study the expression of *At*1g56500 in different plant tissues, *Arabidopsis thaliana* var. Columbia was transformed by the floral dip method (Clough and Bent, 1998) with *Agrobacterium tumefaciens* GV3101 carrying the construct of interest (p*At*GNL:pCAMBIA1305.1). A different set of plants was also transformed with bacteria carrying the empty vector control (pCAMBIA1305.1). T0 seeds were selected with hygromycin and the antibiotic resistant seedlings were transferred to soil and grown to maturity under the above mentioned conditions. The presence of the transgene of interest was established via PCR using gene specific primers, and genomic cDNA as a template. Seeds of the PCR positive plants were sterilized and transferred to a petri dish containing MS media with 20 mg/L hygromycin. Plated seeds were vernalized for 3 days at 4°C and then transferred to an environmentally controlled chamber. Hygromycin resistant seedlings were transferred to soil and grown until maturity.

Explants (seedlings, leaves, flowers, and fruits) were cut from plants 4, 8, 12, and 30 days after germination. Next, the explants were incubated in fresh and cold phosphate buffer pH 7.0 with 4% formaldehyde at room temperature for 30 min. The explants were

washed several times with cold phosphate buffer for 1 h, then vacuum infiltrated with X-Gluc substrate solution containing: 1 mg 5-bromo-4-chloro-3-indolyl β-D-glucuronide in 100 µL of methanol, 1 mL 2X phosphate buffer, 20 µL 0.1 M potassium ferrocyanide, 20 µL 0.1 M potassium ferricyanide, 10 µL 10% (w/v) solution of Triton X-100, and 850 µL of water. Tissues were incubated in darkness at room temperature overnight until a distinct blue staining appeared. Finally, explants were incubated in 70% ethanol until the chlorophyll was removed. Photographs were taken with AxioCam MRc camera connected to a Stemi 2000-C stereo microscope (Zeiss).

2.2.11. Phylogeny

In order to identify a functional GNL in *Arabidopsis thaliana* (*At*GNL), known GNLs, and putative GNLs from other organisms were compared using the TAIR database (www.arabidopsis.org). The *At*GNL was obtained from TAIR database based on highest protein homolog. That sequence was then converted to FASTA format using the EMBL-EBI (www.ebi.ac.uk/tools/stc/readseq/). The MEGA6 software enabled reading and comparing the *At*GNL with known and putative GNL sequences (Tamura *et al.*, 2013).

2.2.12. Statistical analysis

Data was analyzed by SAS software 9.4 (SAS Institute, 2016). Analysis of variance was carried out by ANOVA procedure. Least squares means (LS-means) were calculated to evaluate AsA content per line, at α=0.05.

2.3. Results and Discussion

2.3.1. Purification and characterization of recombinant *At*1g56500

To demonstrate the GNL activity of *Arabidopsis thaliana* gluconolactonase *in vitro*, an *N. benthamiana*-based transient expression system was used. Plants were vacuum infiltrated with the *Agrobacterium tumefaciens* LBA4404 strain carrying the *At*1g56500-6XHIS construct. The protein accumulation is highest at 48 h post infiltration (data not shown).

In order to establish a protein purification protocol for *At*GNL, several extraction buffers were tested to identify those that allow recovery of the highest amount of protein. FIG. 9 shows the list of buffers tested for protein purification.

Protein fractions from the various purification procedures were separated by SDS-PAGE and *At*GNL was detected by Western blot. FIG. 10 shows the *At*GNL protein extracted with different buffers. Western blot of total protein extracted from *N. benthamiana* leaves with different buffers as described in FIG. 7. M: marker, lane 1: crude extract with buffer-1, lane 2: crude extract with buffer-2, lane 3: crude extract with buffer-3, lane 4: crude extract with buffer-4, lane 5: crude extract with buffer-5, lane 6: sample extracted in buffer-5 and resuspended in buffer-4, lane 7: crude extract in buffer-5, lane 8: sample extracted in buffer-5 and resuspended in buffer-3, lane 9: sample extracted in buffer-5 and resuspended in buffer-6, lane 10: crude extract in buffer-6.

The optimal buffer to recover more recombinant protein was buffer 6.

In order to establish the optimal concentration for washing and elution buffer, several imidazole concentrations were tested. FIG. 11 shows the *At*GNL protein eluted with different imidazole concentrations. Western blot of *At*GNL protein with different

concentration of imidazole. M: marker, B6: crude extract in buffer 6, FT flow through, W: wash buffer. As illustrated in FIG. 11, 40 mM and 250 mM were best for washing and eluting conditions, respectively.

FIG. 12 shows the Purification of the *At*GNL:pBIB-kan-6XHIS expressed in *N. benthamiana* leaves. M: marker, lane 1: crude extract, lane 2: flow through, lane 3: wash, lane 4: enzyme, lane 5: concentrated enzyme. FIG. 12 illustrates the result of the purification of *At*GNL from *N. benthamiana* tissue using nickel affinity chromatography. Western blot results showed the presence of *At*GNL in the crude extract and flow through or wash indicating protein had a partial binding to the cation column. The silver-stained gel indicates that the protein preparation contained mostly the protein of interest with a few minor contaminants.

2.3.2. Enzyme activity of recombinant *At*1g56500

Once an effective purification procedure was developed, the next step was to standardize the assay to test the *At*GNL activity. Gluconolactonase (GNL, EC 3.1.1.17) catalyzes the hydrolysis of D-glucono-σ-lactone (D-GulL) to D-gluconic acid (Ogawa *et al.*, 2002). The lactonase activity was assayed *in vitro* based on the decrease in absorbance (405 nm) of the *p*-nitrophenol pH indicator that resulted from the enzymatic opening of the lactone ring when D-glucono-δ-lactone (D-GuIL) was used as substrate in the presence of the *At*GNL as previously described (Hucho and Wallenfels, 1972). The enzymatic activity was assayed at 25°C with 10 mM PIPES pH 6.5, 5 mM D-GuIL, 75 µM $MnCl_2$, 2.5 mM *p*-nitrophenol, and 30 µg of the purified enzyme (*At*GNL) in 1 mL of reaction (Ishikawa *et al.*, 2008).

With the exception of D-GuIL, the recombinant *At*GNL did not exhibit activity with any of the substrates tested. FIG. 13 shows the Substrate preference of *At*GNL.

All enzymes work with a range of temperatures specific to the organism from which they are extracted. The effect of temperature on the *At*GNL activity was also determined. The activity of the *At*GNL enzyme was highest at temperatures between 25°C and 35°C. The activity drastically decreased when the temperature was increased to 40°C. FIG. 14 shows the Effects of temperature and pH on the activity of the *At*GNL enzyme. (**A**) pH effect on GNL activity. (**B**) Temperature effect on GNL activity. Measurements were made in duplicate. Values are means ± SD. Ogawa *et al.*, (2002) reported that the GNL enzyme from *A. niger* had higher activity at 30°C, while the activity of the GNL from *P. aeruginosa* is optimal at 24°C (Tarighi *et al.*, 2008), which are similar to the *At*GNL.

Kondo *et al.*, (2006), reported that the activity of the rat GNL was highest at pH 6.4, while Tarighi *et al.*, (2008) demonstrated that the optimal activity of the *P. aeruginosa* GNL was at pH 7.2. In contrast, in this study the *A. thaliana* GNL enzyme had a higher activity at pH 6.0, and the activity decreased by 4-fold when the pH was increased to 6.3 (FIG. 14). Lower pH values were not tested because PIPES buffer cannot dissolve at pHs lower than 6.0.

To assess if the *At*GNL activity had a preference for a particular divalent ion, various cofactors were tested. Ishikawa *et al.*, (2008) reported that the GNL enzyme from *E. gracilis* had a higher activity using $ZnCl_2$ as a cofactor and that this activity decreased around 4-fold when changed to $MnCl_2$. In these experiments, no significant difference in GNL activity among the tested cofactors was observed (FIG. 15). Increasing the substrate concentration increased the rate of reaction or enzyme activity. In order to identify the

optimal concentration of the D-glucono-δ-lactone, multiple substrate concentrations were tested. FIG. 15 shows the Effects of cofactor and substrate on the activity of the *At*GNL enzyme. (**A**) Cofactors effect on GNL activity. (**B**) D-GuIL substrate concentration effect on GNL activity. Measurements were made in duplicate. Values are means ± SD. The 3 mM of D-glucono-δ-lactone was the most effective substrate concentration for this assay.

Enzyme kinetic analysis was performed with D-GuIL at a concentration of 1 mM to 50 mM of substrate. The enzyme activity with 5 mM of D-GuIL at pH 6.0 was 10.54 μmol min^{-1} mg^{-1} of protein, V_{max} = 1.161 x 10^{-6} (38.7 μmol min^{-1} mg^{-1} of protein) and K_m = 2.989. FIG. 16 shows the Enzyme kinetics of the recombinant *At*1g56500 enzyme. (**A**) Michaelis-Menten. (**B**) Double reciprocal Lineweaver-Burke. Measurements were made in duplicate. Values are means ± SD. FIG. 17 summarizes the comparison between the kinetic parameters of the *At*GNL with the one of known GNLs. Based on these results the *G. oxidans* GNL is the most similar to the Arabidopsis GNL.

2.3.3. Characterization of the phenotype of gluconolactonase lines with a Scanalyzer HTS platform

Seeds expressing the *At*GNL-6XHIS:pBIB-kan (*At*GNL) and empty pBIB-Kan (control) were screened in the Lorence Laboratory (unpublished). One hundred and thirty primary transformants that were PCR positive were screened to identify high AsA expressers. After four rounds of screening, three lines per group were selected for further analysis: over-expressers (WT + *At*GNL), restored 1 (SALK_026172 + *At*GNL), and restored 2 (SALK_011623 + *At*GNL).

Homozygous lines (T5), plants with 100% germination in the presence of antibiotic selection were developed for over-expresser (L60, L61, L62), restored-1 lines (L89, L90, L100), and restored-2 lines (L128, L129, L130). FIG. 18 shows the total foliar AsA level of *At*GNL lines under normal light conditions. (**A**) Over-expressers and wild type (WT). (**B**) Restored lines and knockout control (S_026172). (**C**) Restored lines and knockout control (S_011623). Asterisks indicate significant differences between controls and high AsA lines as determine by Turkey multiple comparisons test, α=1, ****=P<0.0001, ***=P<0.0002, **=P<0.0017, *=P<0.0155. Values are means ± SD, n=15.

The phenotype of these homozygous lines was analyzed using a Scanalyzer HTS instrument under normal conditions as described in materials and methods. Plant images were captured every two days from 16 to 26 days after germination. Representative images of homozygous *At*GNL lines and their respective controls are shown in FIG. 19. From these images the projected leaf area as an indicator of plant growth was measured. FIG. 19 shows the Phenotype of *At*GNL lines grown under normal conditions. (**A**) Representative images of *At*GNL lines acquired with the visible camera (aka RGB). (**B**) Growth curves of *At*GNL lines compared with their respective controls. Values are means ± SE, n=15. There is a strong correlation between higher biomass and projected leaf area. Restored-1 and restored-2 lines had more biomass compared to their controls SALK_026172, SALK_011623, respectively, and those restored lines presented higher projected leaf area compared with their controls.

Based on these results, foliar AsA level, and the phenotype analysis, further studies were done only with the lines that had the highest foliar AsA content and fastest growth and higher biomass and projected leaf area.

Over-expresser L61 (OE) and the empty vector control (EV); restored-1 L100 (R-1) and its control SALK_026172 (KO-1), restored-2 L129 (R-2), and its control SALK_011623 (KO-2), and wild type (WT) control were selected for further analysis. First, the effect of low and high light conditions on the selected plants was assessed. Routinely, plants are grown in environmental control chambers. A first attempt to study light effects was accomplished by growing plants in multiple chambers: (315 = 7 lines x 15 biological replicates x 3 light treatments). However, it was very difficult to achieve uniform conditions, with the only variable being the light intensity. To solve this problem, the experiment was conducted in the greenhouse. Two different density meshes were used to diffuse the light to the plants. FIG. 20 shows the experimental set up for studying the effect of light on the phenotype of *At*GNL lines. Light intensity was measured four times per day (9:00 am, 12:00 pm. 3:00 pm, and 6:00 pm) to cover the sunlight period. The light intensity for these three treatment was defined as: low light (35 – 110 µmol/m^2/s), normal light (110 – 350 µmol/m^2/s), and high light (350 – 700 µmol/m^2/s).

Normal outdoor light on a sunny summer day is around 1000-2000 µmol/m^2/s (Mishra *et al.*, 2012) However, because *A. thaliana* is a spring understory plant, anything above 350 µmol/m^2/s is considered high light.

Fifty mg of leaf tissue were collected at developmental stage 6.3 as defined by Boyes *et al.*, (2001) between 9:00-11:00 am. Reduced, oxidized, and total AsA were measured via an enzyme-based method as previously described (Haroldsen *et al.*, 2011). The results indicate that the over-expresser and the restored lines had a higher foliar AsA than their respective controls growing under similar conditions. FIG. 21 shows the Total foliar AsA levels of *At*GNL lines under low, normal and high light conditions. (**A**) Over-

expressers and wild type (WT). (**B**) Restored lines and knockout control (SALK_026172). (**C**) Restored lines and knockout control (SALK_011623). S026172 had a lower significant difference compared with wild type control at high light treatment. Each line was compared to the control (WT), analyzed by *t*-tests (LDS) at α=0.05. Significant differences are indicated by***. WT: wild type, EV: empty vector, OE: over-expresser, KO: knockout, R: restored. n=15. The statistical analysis of total foliar AsA content in the three different light treatments in AtGNL lines shown in FIG. 22 validates this conclusion. Two-way ANOVA (α=0.05). The table in FIG. 22 indicates lines are significantly different and that there is a significant interaction between the lines and light treatments.

The projected leaf area results showed the same trend, where over-expressers and restored lines were bigger than their controls, with KO-1 being the worst performer at all light conditions tested. FIG. 23 shows the Projected leaf area of *At*GNL lines grown under low, normal, high light conditions. (**A**) Low light. (**B**) Normal light. (**C**) High light. Values are means of 15 biological replicates. WT: wild type, EV: empty vector, OE: over-expresser, KO: knockout, R: restored. n=15. There is a strong correlation between foliar AsA level and projected leaf area: over-expresser and restored lines had higher foliar AsA levels and higher projected leaf area compared with their respective controls.

In planta chlorophyll, fluorescence measured with the fluorescence camera can serve as an indicator of whether the plants are under stress. These plants were grown under the normal light regime. High fluorescence in plants is opposite of high photosynthetic efficiency (Lichtenthaler, 1988). FIG. 24 shows the Chlorophyll fluorescence patterns of *At*GNL lines. Relative *in planta* chlorophyll content measured with the FLUO camera. Values are means of 15 biological replicates. WT: wild type, EV: empty vector, OE: over-

expresser, KO: knockout, R: restored. n=15. The knockout KO-1 line showed high fluorescence compared to the other lines under high light conditions. This knockout line has a lower AsA level in the leaves, lower biomass, and projected leaf area, and also higher fluorescence compared with rest of the lines. Overall these results show that the *At*GNL enzyme is essential to support normal AsA content in leaves and normal growth and development in Arabidopsis.

2.3.4. Photosynthetic efficiency of *At*GNL lines under low and normal light conditions

Genes involved in the AsA metabolic network have been identified that were down and up regulated in response to light. FIG. 25 shows the Effect of darkness on the expression of genes in the AsA metabolic network. Microarray data deposited at Genevestigator was mined. Genes that are down regulated in darkness are shown in red, while genes that are up-regulated are shown in green. Yellow color indicates genes isoforms that are upregulated under dark conditions. The D-mannose/L-galactose, L-gulose and D-glucuronate pathway are repressed under low light conditions while the *myo*-inositol pathway keeps working. Suza and Lorence, unpublished. These results indicate that the L-gulose, D-mannose/L-galactose, and D-galacturonate pathways are down regulated under darkness, while the *myo*-inositol route is up regulated. If the transcripts are down regulated, the enzymes are expected to be down regulated as well. Because photosynthetic efficiency is a measure of light stress and redox potential, photosynthetic efficiency was analyzed for *At*GNL lines growing under low and normal light conditions. These photosynthetic

efficiency measurements were done with a MultispeQ, a hand-held device developed in the Kramer Laboratory (Michigan State).

Photosynthetic efficiency is the fraction of light (photons) that plants obtain from the sun to convert into chemical energy during photosynthesis. Under normal light conditions there was no penalty in the photosynthetic efficiency of plants lacking *AtGNL* expression. FIG. 26 shows the Photosynthetic efficiency of *At*GNL lines under low and normal light conditions. Each line was compared to the control (WT), analyzed by *t*-tests (LDS) at α=0.05. Significant differences are indicated by ***. WT: wild type, EV: empty vector, OE: over-expresser, KO: knockout, R: restored. n=10. In contrast, the over-expressers and restored lines displayed enhanced efficiency indicating a positive impact on photosynthesis due to higher *AtGNL* expression. When plants were grown under low light, results were quite different. In this case a lower photosynthetic efficiency was detected in EV and KO-1 compared to the WT control. This indicates a penalty in photosynthetic efficiency due to lack of *AtGNL* expression. FIG. 27 shows the Statistical analysis of photosynthetic efficiency of *At*GNL lines grew at low and normal light conditions. Two-way ANOVA (α=0.05). Photosynthetic efficiency as response to light conditions. The table indicates the treatment light has a significant effect pvalue=0.001. The lines also has a significant effect pvalue<0.0001, and there is a significant interaction between light and lines pvalue=0.1773.

In addition to photosynthetic efficiency two other parameters related to photosynthesis were measured: linear electron flow (LEF) and non-photochemical quenching (NPQt). The linear electron flow rate (LEF) has a direct correlation to photosynthetic efficiency. LEF facilitates the movement of H^+ ions across the thylakoid

membrane to create an electrochemical gradient that is used by ATP-synthase to produce energy (ATP). FIG. 28 shows the Linear electron flow of *At*GNL lines under low and normal light conditions. Each line was compared to the control (WT), analyzed by *t*-tests (LDS) at α=0.05. Significant differences are indicated by ***. WT: wild type, EV: empty vector, OE: over-expresser, KO: knockout, R: restored. n=10. FIG. 28 shows that under low light conditions both knockouts had lower LEF values than the controls, while KO-1 was the line with the worst performance under normal light conditions. FIG. 29 shows the Statistical analysis of linear electron flow of *At*GNL lines grown at low and normal light conditions. Two-way ANOVA (α=0.05). LEF as response to light conditions. The table indicates the treatment light has a significant effect pvalue=0.0006. The lines also has a significant effect pvalue<0.0001, and there is a significant interaction between light and lines pvalue=0.0091. These data highlights the importance of the *At*GNL enzyme for efficient ATP production in the chloroplasts.

Plants exhibit phenotypic plasticity and respond to differences in environmental conditions by acclimation. In a recent study, Arabidopsis plants grown under field conditions were compared with plants grown indoors. Indoor-grown plants had larger leaves, modified leaf shapes and longer petioles and less NPQt, while field-grown plants had a high capacity to perform state transitions (Mishra *et al.*, 2012). If photosynthesis is inefficient, excess light energy is dissipated as heat to avoid damaging the photosynthetic apparatus. When plants are under abiotic stress, such as low light intensity, the photosynthetic efficiency and the NPQt are opposite. The KO-1 line had high NPQt, indicating inefficient photosynthesis at both low and normal light conditions. FIG. 30 shows the Non-photochemical quenching coefficient of *At*GNL lines under low and normal

light conditions. Each line was compared to the control (WT), analyzed by *t*-tests (LDS) at α=0.05. Significant differences are indicated by ***. WT: wild type, EV: empty vector, OE: over-expresser, KO: knockout, R: restored. n=10. Statistical analysis indicates the KO-1 line had a highly significant difference compared to the WT control. FIG. 31 shows the Statistical analysis of non-photochemical quenching of *At*GNL lines grown at low and normal light conditions. Two-way ANOVA (α=0.05). Non-photochemical quenching as response to light conditions. The table indicates the treatment light has a significant effect pvalue=0.001. The lines also has a significant effect pvalue<0.0001, and there is a significant interaction between light and lines pvalue=0.4475. Overall, the over-expressers, restored lines, wild type, and empty vector lines had higher values of photosynthetic efficiency and LEF compared with KO lines under normal and low light conditions, while the NPQt values were opposite with the KO-1 having the highest value. These results show that *At*GNL expression is essential to maintain high photosynthetic efficiency, high electron flow to make ATP (high LEF) and less loss of energy in the form of heat (NPQt).

2.3.5. Temporal and spatial expression of *At*GNL using the GUS reporter gene

To examine the expression of *At*GNL within tissues, ten transgenic plants expressing GUS driven by the *At*GNL promoter (p*At*1g56500:pCAMBIA1305.1) and empty vector pCAMBIA1305.1 (control) were generated. In the empty vector the *GUS-PLUS* gene is under the control of the 35S constitutive promoter.

*At*GNL, empty vector and wild type plants were treated with the X-Gluc substrate. As illustrated in FIG. 32 GUS activity was evident in plants expressing the *At*GNL promoter in all developmental stages from cotyledons to roots, although much less staining

was observed in 4-day-old seedlings compared with the controls. The oldest seedlings stained most intensely, especially at the leaf tips and margins. FIG. 32 shows the Temporal and spatial expression of *At*GNL using the *GUS-PLUS* reporter gene. The *At*GNL is expressed in the whole plant and at all developmental stages, indicating that the GNL enzyme is important in the physiological development of the plant from beginning to maturity.

2.3.6. Phylogenetic three of putative plant gluconolactonases

A phylogenetic tree for *At*1g56500 (*At*GNL) was generated. *At*1g56500 (*At*GNL) was compared with known GNLs and with putative GNLs for many other organisms. After all protein sequences with significant sequence similarity to *At*GNL were retrieved, the protein sequences were aligned using the MEGA6 software (Tamura *et al.*, 2013). Only the sequences that had between 90 and 100% of identity with the *At*GNL protein of interest were included in this analysis. To develop an updated phylogenetic tree, a BLASTP search was done against the Arabidopsis protein database (www.arabidopsis.org) using the *A. thaliana* gluconolactonase "*At*1g56500" (*At*GNL) protein sequence. This enzyme has been characterized in *A. niger* (Ogawa *et al.*, 2002), *E. gracillis* (Ishikawa *et al.*, 2008), *P. aeruginosa* (Tarighi *et al.*, 2008), *R. norvegicus* (Kondo *et al.*, 2006), *Z. mobilis* (Pedruzzi *et al.*, 2007), and now also in Arabidopsis (this work). The BLASTP result revealed the presence of 37 candidates in different organisms with 90-100% identity to the *At*GNL query. FIG. 33 shows the Phylogenetic analysis of known and putative GNLs. Phylogenetic analyses were conducted in MEGA6 (Tamura *et al.*, 2013). Five branches can be distinguished in this phylogenetic tree where the *At*GNL groups with proteins from plant

species including plant crops of agricultural importance including *Cucumis sativus* (cucumber), *Cucumis melo* (melon), *Citrus sinensis (orange), Vitis vinifera* (grapes), *Theobroma cacao* (cacao), *Glycine max* (soybean), and *Fragaria vesca* (strawberry), trees such as *Populus trichocarpa* (poplar) and *Prunus mume (Chinese plum),* and energy crops such as *Jatropha curcas*. The sequence similarity between *At*1g56500 and putative GNLs from other plants is remarkable. In a second group we can see known GNLs from mammalian species including *R. novergicus*, *H. sapiens*, and putative GNLs from *Ovis aries*, *Canis familiaris* and others. In the third and fourth branches we can see known and putative GNLs from bacteria and fungi. In a fifth group we find putative GNLs from *A. thaliana*. The analyses showed that *At*1g56500 has high similarity with the protein sequences listed in FIGS. 34A and 34B. Figures 34A and 34B show the List of known and putative GNLs included in the phylogenetic analysis. Underlined species indicate the GNL enzymes that have been characterized biochemically.

The constitutive expression of the gene of interest (GNL) leads to higher seed yield in plants, such as Arabidopsis. Such higher seed yield is shown in FIG. 35.

FIG. 36 shows the GNL DNA sequence.

FIG. 37 shows the GNL amino acid sequence. In one embodiment, the GNL over-expressed in the plant may include at least 70% of the sequence shown in FIG. 36 or FIG. 37.

2.4. Conclusions

The evidence presented in this document allows the following conclusions:

We successfully developed a purification protocol for *At*GNL recombinant protein, and characterized this enzyme in detail including temperature, pH, cofactor requirement, and substrate concentration preferences, as well as its kinetic parameters.

The *At*GNL enzyme had highest activity at temperatures between 25°C to 35°C, while the bacteria *P. aeruginosa* has optimal temperature activity at 24°C. The optimum temperature of the *At*GNL is consistent with the preferred growth temperature of Arabidopsis.

The optimal pH for *At*GNL enzymatic activity was 6.0, and this activity decreased 4X when the pH was slightly increased (pH 6.3). In contrast, mammalian GNLs isolated from rats, mice, and humans have an optimal activity at pH 6.4. Our result is consistent with the prevalent pH in the chloroplasts (Alberts *et al.*, 2002), the organelle where this protein resides.

The enzyme characterized in this work is very specific with the D-GuIL substrate. In contrast the recombinant GNLs from *E. gracilis* and *R. norvegicus* are promiscuous as they displayed activity with additional substrates (Kondo *et al.*, 2006; Ishiwaka *et al.*, 2008b).

GNL enzymes require a divalent cofactor for activity. The *At*GNL displayed similar activity when incubated with $MnCl_2$, $MgCl_2$, or $ZnCl_2$. In contrast, other GNLs such as the *E. gracilis* isoform prefer $ZnCl_2$ and activity dropped significantly with other cofactors (Ishikawa *et al.*, 2008). The ability of *At*GNL to work with $MnCl_2$ is consistent with an enzyme that is active in the chloroplasts, as Mn is abundant in that organelle (Alberts *et al.*, 2002).

Based on optimum pH, optimum T, and kinetic parameters of the known GNLs the one that is the most similar to the one here characterized is the *G. oxydans* GNL.

After demonstrating GNL enzyme activity *in vitro*, the present invention provides a method of controlling the role of this enzyme in AsA biosynthesis *in planta*. As shown in FIG. 18 when constitutively expressed in wild type, this enzyme leads to over-expressers with up to 3-fold increase in foliar AsA content. Two T-DNA insertion knockouts in this gene (SALK lines) had reduced AsA content compared to the WT control. When the functional gene was inserted into the knockout background this led to plants with restored AsA content. Overall this data indicates that *At*GNL is functional *in planta*.

Previous results in the Lorence Laboratory obtained using manual phenotyping showed that plants with high AsA accumulate more biomass, delayed aging and are tolerant to abiotic stresses (Lisko *et al.*, 2013). To determine if the *At*GNL lines display differences in growth rate and biomass accumulation, a powerful high throughput phenotyping instrument was used to characterize the phenotype of lines with normal (WT), low (knockouts) and high (over-expresser and restores lines) GNL expression. A clear penalty in the growth rate and biomass accumulation of the knockouts exists. The restored lines grew as well or better than the controls. This result indicates that *At*GNL is key to the plant to support normal growth and development.

Based on the fact that *At*GNL is a chloroplastic enzyme (FIG. 7), to gain insights about the physiological role of this protein in supporting the function of this organelle, the ability of plants with low, normal, and high *At*GNL expression to adapt to light stress conditions was analyzed. It is well established that there is higher ROS production during low and high light exposure (Sharma *et al.*, 2012). Arabidopsis over-expressers and

restored lines where *At*GNL expression is enhanced display higher AsA content compared to controls.

Detailed characterization of the phenotype of the *At*GNL lines under normal, low and high light conditions showed that over-expressers and restored lines grew better and accumulated more biomass than their respective controls (FIG. 23). The line with the poorest performance was KO-1, the genotype with the lowest AsA content. Interestingly in planta chlorophyll fluorescence analysis show that KO-1 displayed high chlorophyll fluorescence, an indicator of stress. Further analysis will have to be done to determine why KO-1 has a stronger phenotype compared to KO-2.

Plant growth and yield depend on plants maintaining high photosynthetic efficiency. To determine if the stunted growth we measured in the knockouts is due to deficiencies in photosynthesis, measurements were done with a hand-held fluorometer. Interestingly, results show that over-expressers and restored lines displayed enhanced photosynthesis compared to controls, while KO-1 and KO-2 have decreased LEF and therefore decreased ability to make ATP. Overall KO-1 display the poorest performance for all photosynthetic parameters here measured including non-photochemical quenching.

In order to analyze the expression of the *At*GNL in plants tissues we developed transgenic *A. thaliana* lines expressing the *GUS-PLUS* reporter gene under the control of the *At*GNL promoter (p*At*GNL). The results show that *At*GNL is expressed in all tissues examined: seedlings, leaves, stems, and siliques, except roots. This expression pattern suggests that *At*GNL is a constitutive enzyme.

*At*GNL is an important enzyme to sustain sufficient AsA content and to maintain plant growth and efficient photosynthesis. In order to gain insights about the conservation

of this enzyme in evolution, a phylogenetic tree of known and putative GNLs was developed (FIG. 33). At least 37 candidates with 90 – 100% sequence identity to the *At*GNL at the amino acid level exist. This analysis indicates the presence of GNLs in a wide array of plants including crops of agricultural importance, mammals, bacteria, and fungi. Interestingly it appears to be a GNL in *Sellaginella moellendorffii*, an ancient vascular plant that is widely used as a model to study the evolution of plants as a whole (Banks *et al*., 2011).

From the foregoing, it will be seen that the present invention is one well adapted to obtain all the ends and objects herein set forth, together with other advantages which are inherent to the structure.

It will be understood that certain features and sub-combinations are of utility and may be employed without reference to other features and sub-combinations. This is contemplated by and is within the scope of the claims.

As many possible embodiments may be made of the invention without departing from the scope thereof, it is to be understood that all matter herein set forth or shown in the accompanying drawings is to be interpreted as illustrative and not in a limiting sense.

CLAIM OR CLAIMS

What is claimed is:

1. A method of increasing production of L-ascorbic acid (ASA) in a plant or enhancing the photosynthetic capacity of the plant or enhancing the seed yield of the plant, the method comprising:

increasing the level of ASA in the plant by expressing gluconolactonase (GNL).

2. The method of claim 1 further comprising:

Over-expressing the GNL.

3. The method of claim 1 wherein the plant exhibits increased production of ASA.

4. The method of claim 1 where the plant exhibits enhanced photosynthetic capacity and/or enhanced seed yield.

5. The method of the claim 1 wherein the GNL is *At*1g56500.

6. The method of claim 2 wherein the plant is *Arabidopsis.*

7. A method for increasing production of L-ascorbic acid (ASA) or enhancing the photosynthetic capacity of the plant or enhancing the seed yield of the plant, the method comprising:

genetically engineering said plant to over-express a gluconolactonase (GNL) wherein overexpression of said GNL in said genetically engineered plant results in increased vitamin C content in said genetically engineered plant as compared to a control plant of the same species lacking said over-expressing said GNL.

8. The method of claim 6 wherein said step of genetically engineering includes i) isolating and purifying the GNL; and ii) transforming said plant with said GNL.

9. The method of claim 8 wherein said step of genetically engineering said plant results in increasing production of ASA compared to a control plant of the same species lacking the GNL.

10. The method of claim 8 wherein said step of genetically engineering said plant results in enhancing the photosynthetic capacity of the plant and/or enhanced seed yield of the plant compared to a control plant of the same species lacking said over-expressing GNL.

11. The method of the claim 7 wherein the GNL is *At*1g56500.

12. The method of the claim 9 wherein the GNL is *At*1g56500

13. The method of the claim 10 wherein the GNL is *At*1g56500

14. The method of claim 9 wherein the plant is *Arabidopsis.*

15. The method of claim 10 wherein the plant is *Arabidopsis*.

16. A plant genetically engineered to over-express a gluconolactonase (GNL), the plant comprising:

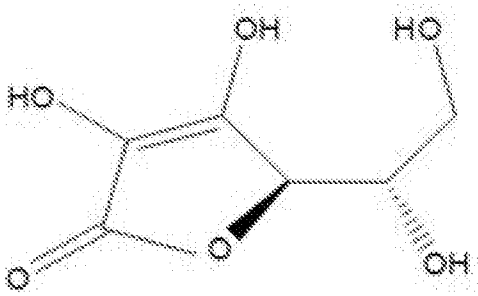
Over-expressed GNL wherein said genetically engineered transgenic plant has increased vitamin C content as compared to a control plant of the same species lacking the GNL.

17. The plant of claim 16 wherein said plant exhibits increased production of ASA compared to a control plant of the same species lacking the GNL.

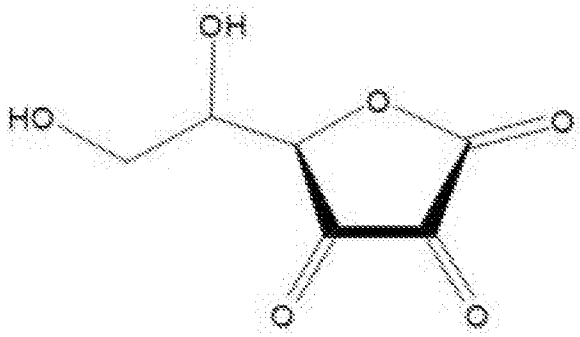
18. The method of claim 16 wherein said plant exhibits increased seed yield compared to a control plant of the same species lacking the GNL.

19. The plant of claim 16 wherein the GNL is *At*1g56500

20. The plant of claim 16 wherein the plant is *Arabidopsis*.



L-Ascorbic acid
Reduced form
$C_6H_8O_6$
Mol. Wt.: 176.12



Dehydroascorbic acid
Oxidized form
$C_6H_6O_6$
Mol. Wt.: 174.11

FIG. 1

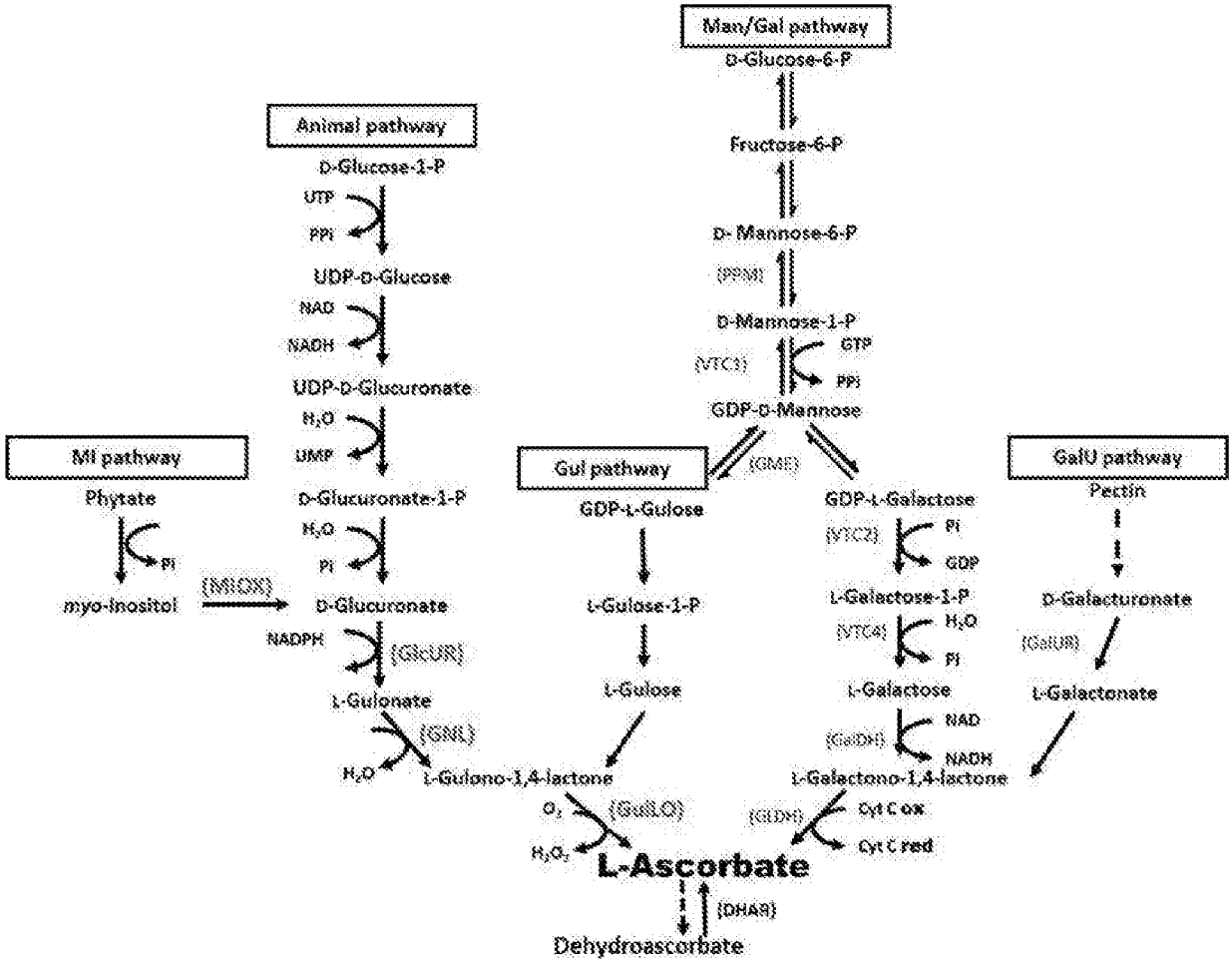

Man/Gal pathway
D-Glucose-6-P
Fructose-6-P
D- Mannose-6-P
(PPM)
D-Mannose-1-P
(VTC1)
GTP
PPi
GDP-D-Mannose
Animal pathway
D-Glucose-1-P
UTP
PPi
UDP-D-Glucose
NAD
NADH
UDP-D-Glucuronate
H2O
UMP
D-Glucuronate-1-P
H2O
Pi
MI pathway
Phytate
Pi
myo-Inositol
(MIOX)
D-Glucuronate
NADPH
(GlcUR)
L-Gulonate
(GNL)
H2O
L-Gulono-1,4-lactone
Gul pathway
(GME)
GDP-L-Gulose
L-Gulose-1-P
L-Gulose
GDP-L-Galactose
(VTC2)
Pi
GDP
L-Galactose-1-P
(VTC4)
H2O
Pi
L-Galactose
(GalDH)
NAD
NADH
L-Galactono-1,4-lactone
GalU pathway
Pectin
D-Galacturonate
(GalUR)
L-Galactonate
O2
(GulLO)
H2O2
(GLDH)
Cyt C ox
Cyt C red
L-Ascorbate
(DHAR)
Dehydroascorbate

FIG. 2

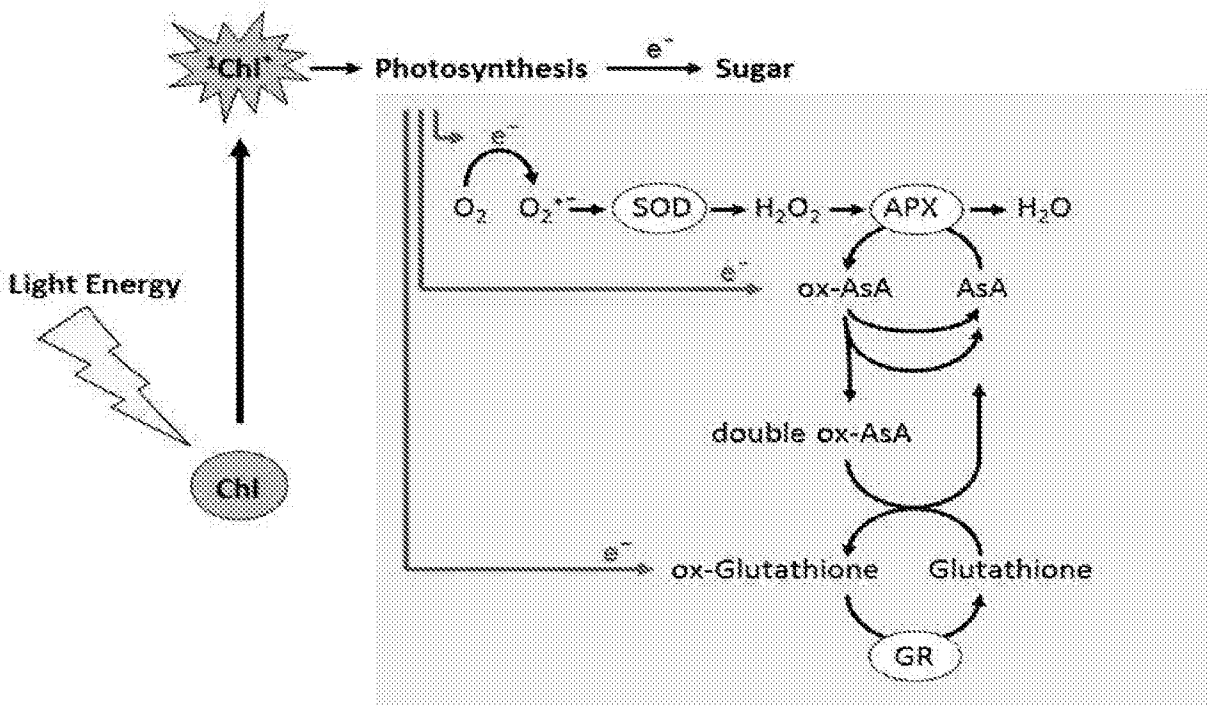

Chl
Photosynthesis
e⁻
Sugar
Light Energy
Chl
O2
O2•⁻
SOD
H2O2
APX
H2O
ox-AsA
AsA
double ox-AsA
ox-Glutathione
Glutathione
GR

FIG. 3

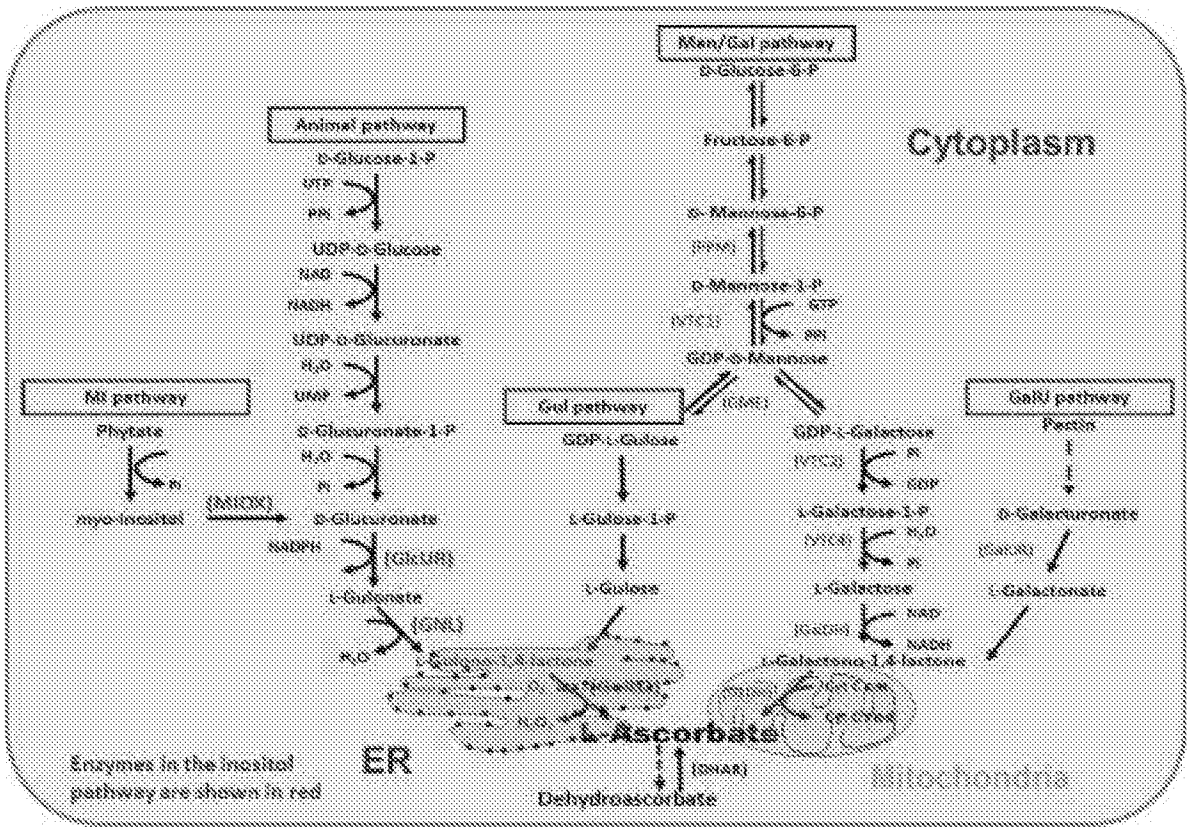

Man/Gal pathway
D-Glucose 6-P
Fructose 6-P
Cytoplasm
Animal pathway
D-Glucose 1-P
UTP
PPi
UDP-D-Glucose
NAD
NADH
UDP-D-Glucuronate
H2O
UMP
D-Glucuronate-1-P
H2O
Pi
MI pathway
Phytate
Pi
myo-Inositol
D-Glucuronate
NADPH
(GLUR1)
L-Gulonate
(GNL)
H2O
D-Mannose-6-P
(PMM)
D-Mannose-1-P
GTP
(GMP)
GDP-D-Mannose
Gal pathway
(GME)
GDP-L-Galactose
GDP-L-Gulose
L-Gulose-1-P
L-Gulose
L-Galactose-1-P
Pi
GDP
H2O
Pi
L-Galactose
NAD
NADH
L-Galactono-1,4-lactone
GalU pathway
Pectin
D-Galacturonate
(GALUR)
L-Galactonate
L-Ascorbate
(GULLO)
Dehydroascorbate
Enzymes in the inositol pathway are shown in red
ER
Mitochondria

FIG. 4

N°	Locus	Knockout	Predicted Localization	Notes
1	*At*1g08470	SALK_055631	NA	Strictosidine synthase family protein
2	***At*1g56500**	**SALK_011623 SALK_026172**	**Chloroplast**	**Haloacid dehalogenase-like hydrolase family**
3	*At*1g74000	SALK_032305	Cell wall	Encondes a protein similar to strictosidine synthase
4	*At*1g74020	SALK_001853	Endomembrane system	Responds to JA; strictosidine synthase family protein
5	*At*2g01410	SALK_147211	Endomembrane system	Expressed protein; AsA
6	*At*2g16780	SALK_001214	NA	WD-40 repeat protein (MSI2), contains 5 WD-40 repeats (PF0400)
7	*At*2g24130	SALK_025037	Endomembrane system	Leucine-rich repeat transmembrane protein kinase, putative
8	*At*2g41290	SALK_015649	Endomembrane system	Strictosidine synthase family protein
9	*At*2g41300	SALK_009989	Endomembrane system	Strictosidine synthase family protein
10	*At*3g51420	SALK_026466	Endomembrane system	Strictosidine synthase family protein
11	*At*3g51430	SALK_055182	Endomembrane system	Strictosidine synthase
12	*At*3g51440	SALK_057855	Endomembrane system	Strictosidine synthase family protein
13	*At*3g51450	SALK_124438	Endomembrane system	Strictosidine synthase family protein
14	*At*3g57010	SALK_091299	Endomembrane system	Strictosidine synthase family protein
15	*At*3g57020	NA	Endomembrane system	Strictosidine synthase family protein
16	*At*3g57030	SALK_120135	Cell wall	Strictosidine synthase family protein
17	*At*3g59530	SALK_033871	Endomembrane system	Strictosidine synthase family protein
18	*At*5g22020	SALK_042799	Endomembrane system	Strictosidine synthase family protein

FIG. 5

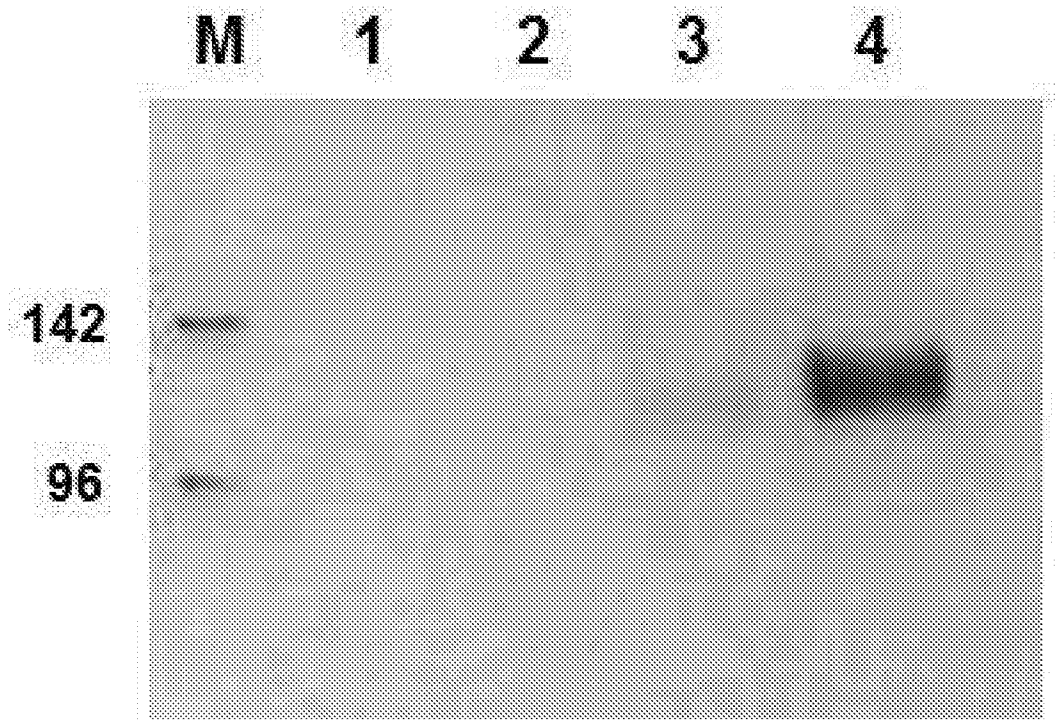
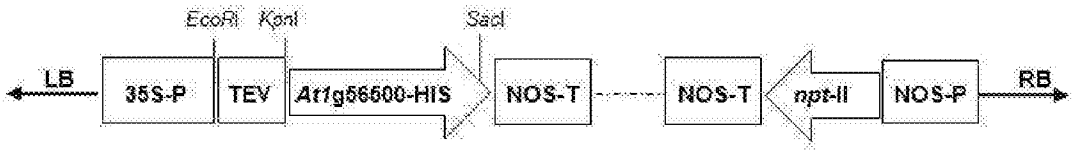


FIG. 7

A. *At*1g56500-HIS:pBIB-Kan



B. p*At*1g56500:pCAMBIA1305.1

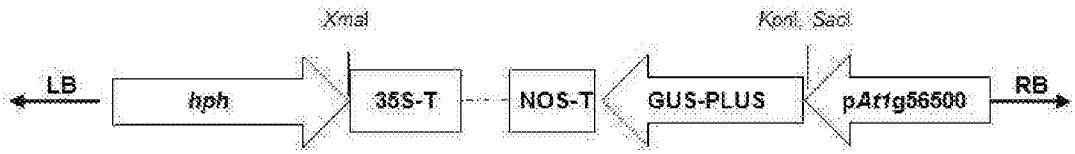


FIG. 8

N°	Buffers	Ref
1	50 mM sodium phosphate pH 7.2, 0.6% protease inhibitor cocktail	Lorence Laboratory
2	50 mM sodium phosphate pH 7.2, 150 mM NaCl, 0.1% Tween-20, 0.6% protease inhibitor cocktail	Lorence Laboratory
3	50 mM Tris-HCl pH 8.0, 0.6% protease inhibitor cocktail	Lorence Laboratory
4	50 mM Tris, 150 mM $MgCl_2$, 10 mM sodium metabisulfite, 0.1% Tween-20, 0.6% protease inhibitor cocktail	Reichel and Beachy, 1998
5	50 mM MES-NaOH pH 6.0, 0.6% protease inhibitor	Lorence Laboratory
6	75 mM sodium phosphate dibasic, 25 mM sodium phosphate monobasic, 300 mM NaCl, 10 mM sodium metabisulfite, 0.6% protease inhibitor cocktail	Lorence Laboratory

FIG. 9

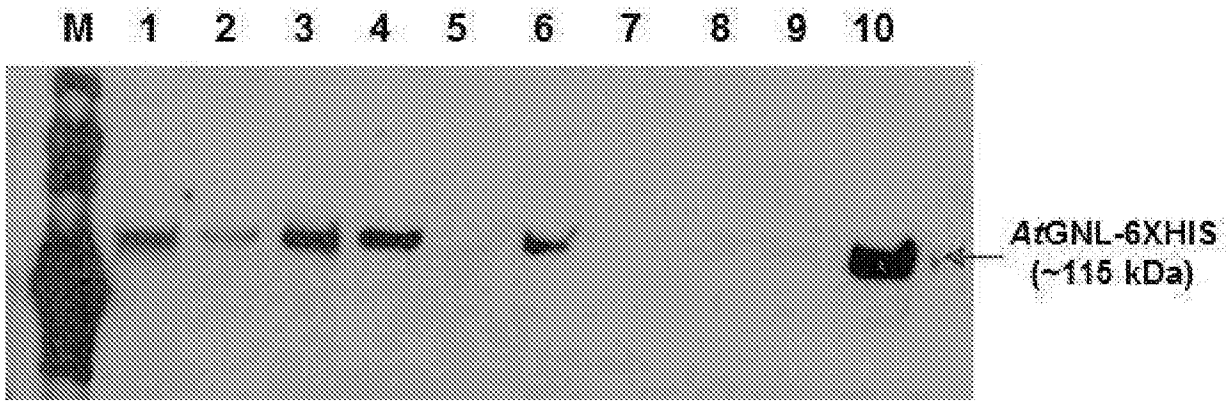


FIG. 10

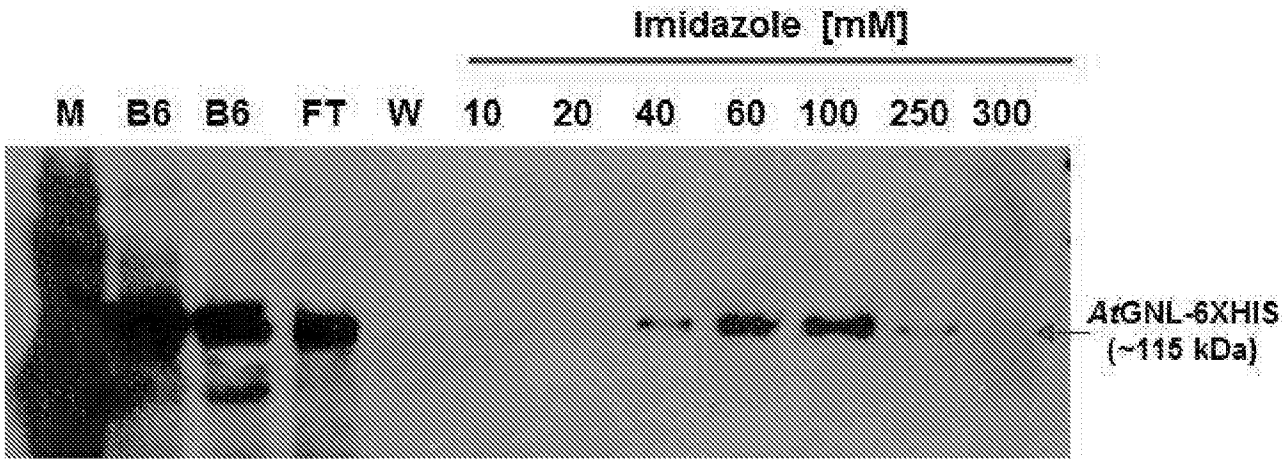

Imidazole [mM]
M
B6
B6
FT
W
10
20
40
60
100
250
300
AtGNL-6XHIS
(~115 kDa)

FIG. 11

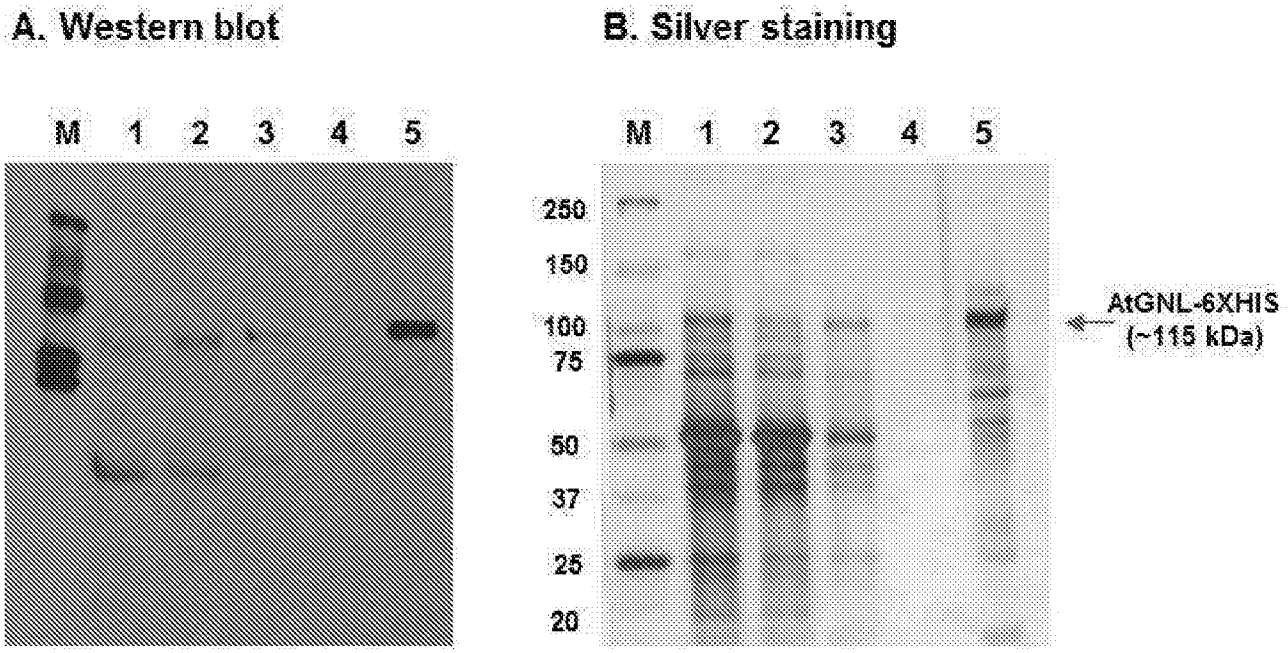

A. Western blot
M 1 2 3 4 5
B. Silver staining
M 1 2 3 4 5
250
150
100
75
50
37
25
20
AtGNL-6XHIS
(~115 kDa)

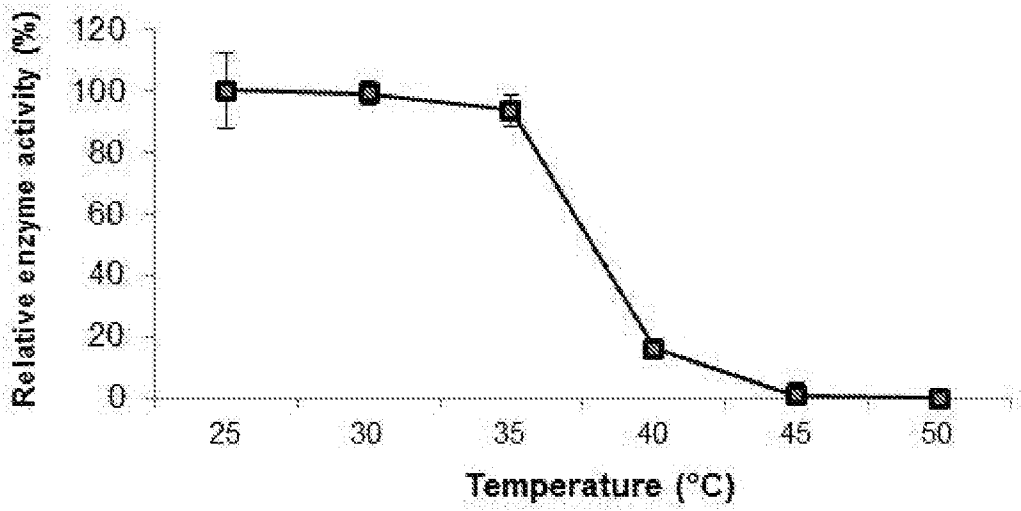
FIG. 12

Substrate[a]	Rate[b] (%)
D-Glucono-δ-lactone	100
L-Galactono-ϒ-lactone	ND
L-Galactonic acid	ND
L-Gulono-ϒ-lactone	ND
L-Gulonic acid	ND

[a]Concentration of substrate was 5 mM. [b]Enzyme activity was determined under standard reaction conditions as defined in "Materials and methods" using the lactonase activity assay, 30 μg of enzyme, and the indicated substrate. ND: no detectable enzyme activity.

FIG. 13

A. Temperature



B. pH

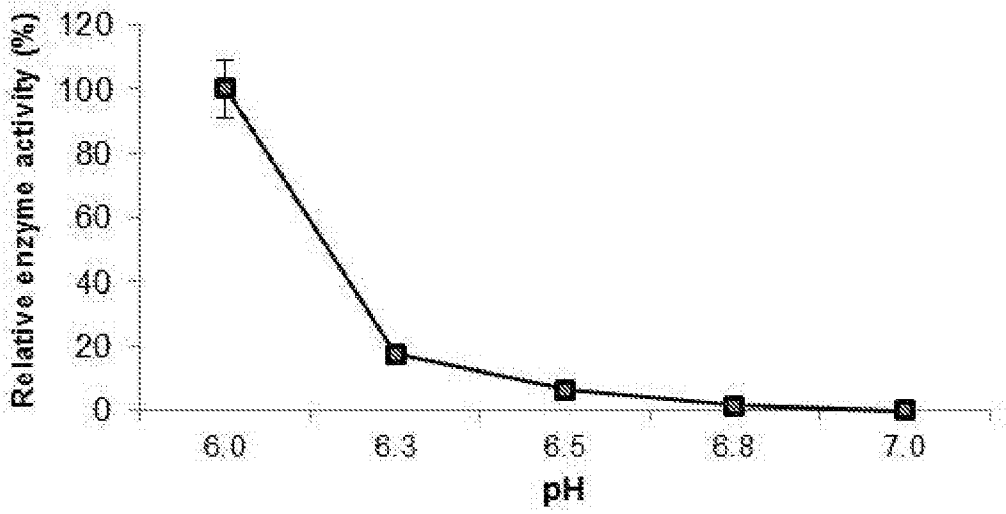
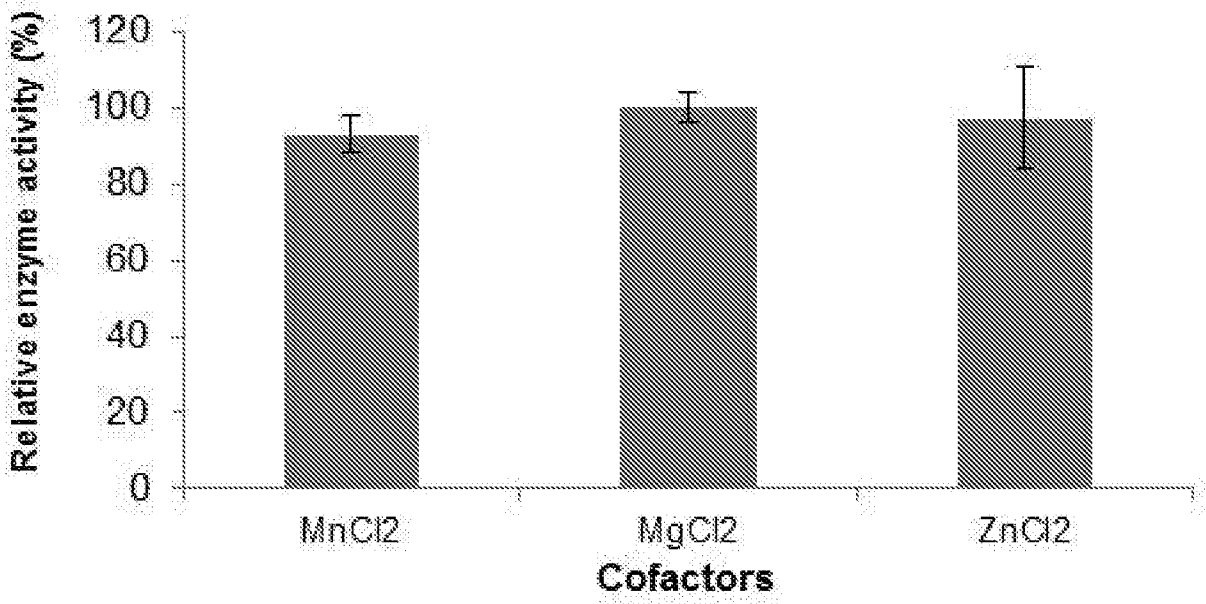


FIG. 14

A. Cofactor



B. Substrate concentration

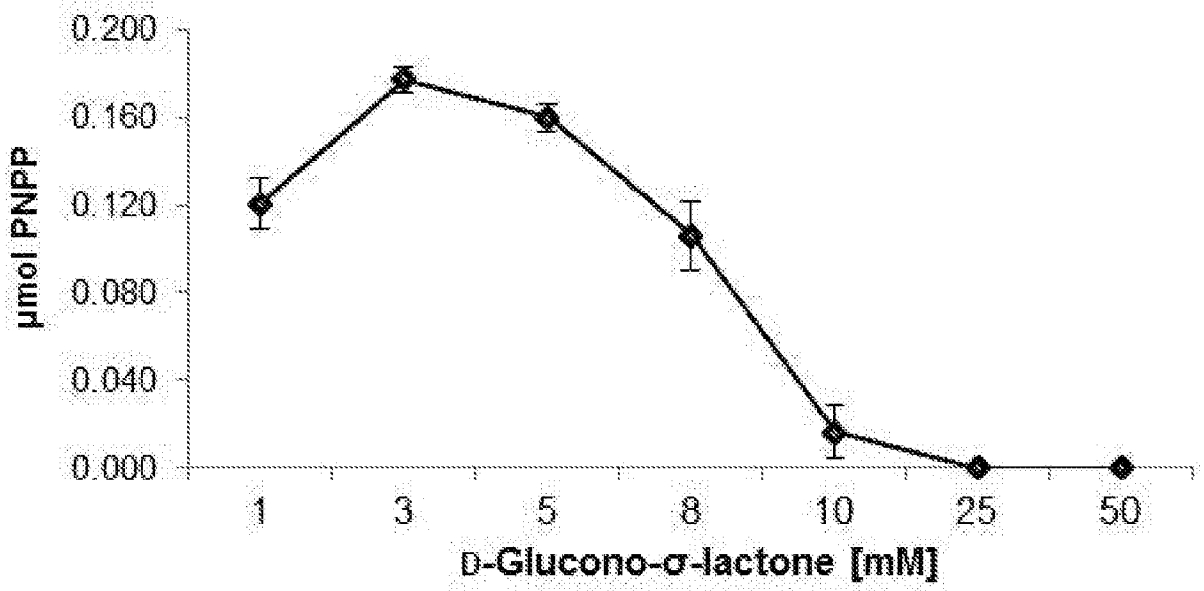
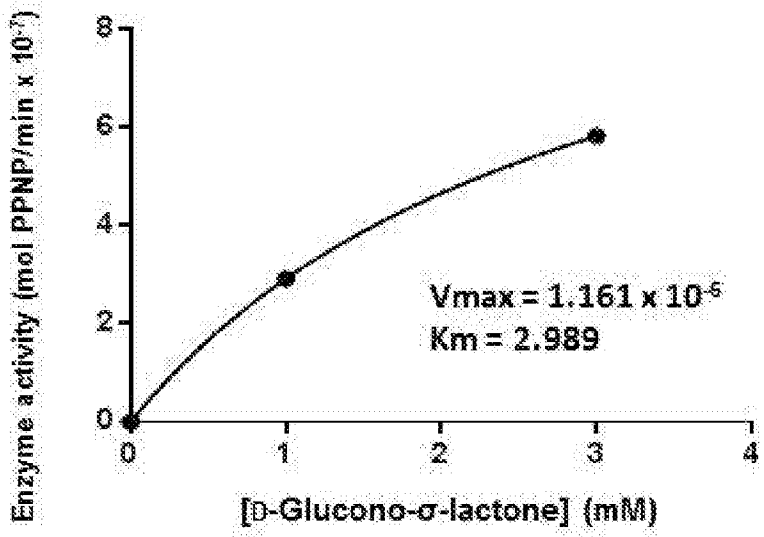


FIG. 15

A. Michaelis-Menten



B. Double reciprocal Lineweaver-Burke

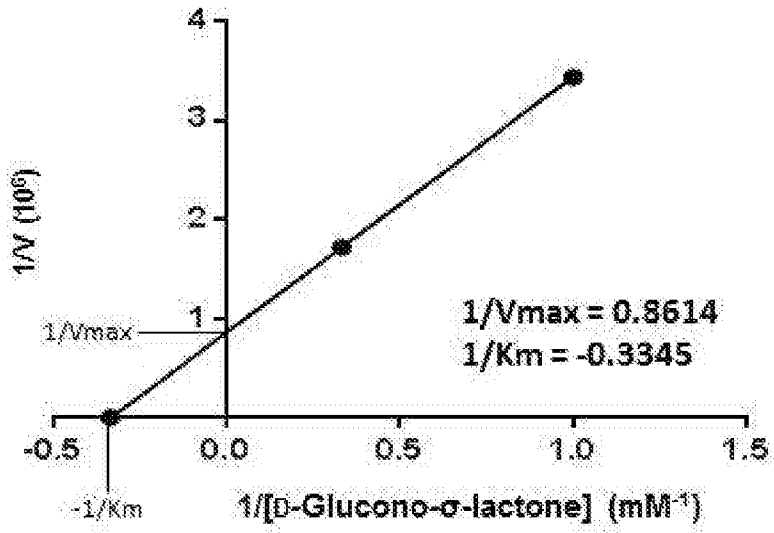


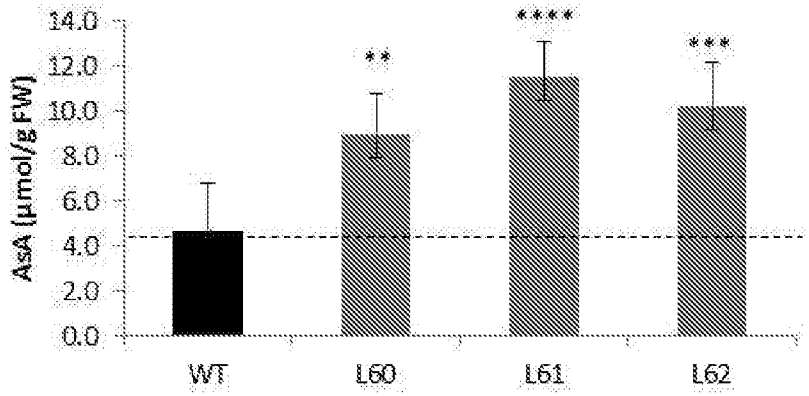
FIG. 16

Species	pH	Cofactor	Specific activity (μmol min^{-1} mg^{-1} of protein)	Km (mM)	Vmax (μmol min^{-1} mg^{-1} of protein)	Ref
Arabidopsis thaliana	6.0	Mn^{+2}, Mg^{+2}, Zn^{+2}	10.54	3	38.7	This work
Rattus novergicus	6.4	Zn^{2+}	9	9.4	345	Kondo *et al.*, 2006
Euglena gracilis	6.5	Zn^{2+}	39	9.4	345	Ishikawa *et al.*, 2008
Pseudomonas aeruginosa	7.2	not mentioned	not mentioned	not mentioned	not mentioned	Tarighi *et al.*, 2008
Xanthomonas campestri	7.0	Ca^{2+}	not mentioned	16.2	160	Chen *et al.* 2009
Gluconobacter oxydans	6.0	Ca^{2+}	not mentioned	2.5	25	Shinagawa *et al.*, 2009
*Homo sapiens (SMP30)**	6.4	Ca^{2+}	25	not mentioned	not mentioned	Aizawa *et al.*, 2013
Mus musculus	6.4	Ca^{2+}	8.8	not mentioned	not mentioned	Aizawa *et al.*, 2013

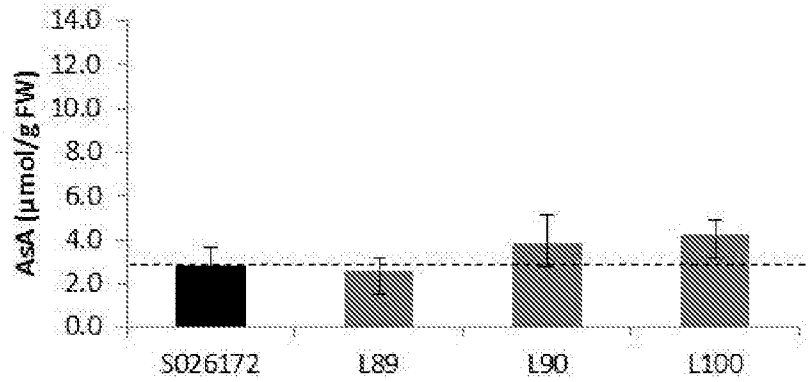
*The human GNL a.k.a. senescence marker protein 30 or SMP30 is a protein whose tissue levels in the liver, kidney and lung decrease with aging.

FIG. 17

A. Over-expresses: WT + *At*GNL



B. Restored lines: SALK_026172 + *At*GNL



C. Restored lines: SALK_011623 + *At*GNL

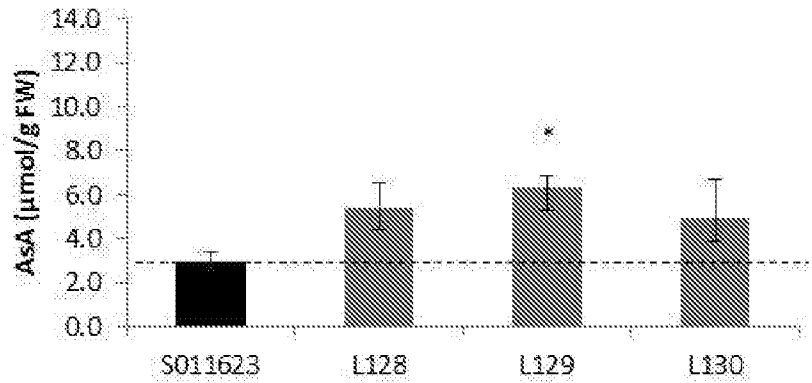


FIG. 18

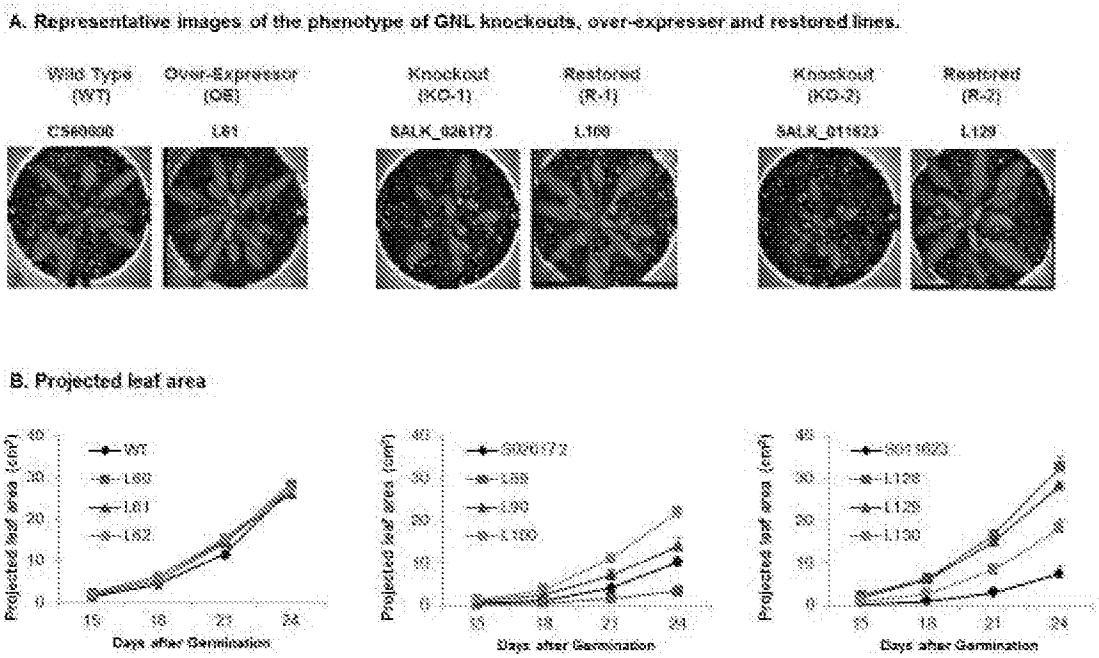

A. Representative images of the phenotype of GNL knockouts, over-expresser and restored lines.
Wild Type (WT)
Over-Expresser (OE)
Knockout (KO-1)
Restored (R-1)
Knockout (KO-2)
Restored (R-2)
L61
SALK_026172
L100
SALK_011623
L129
B. Projected leaf area
WT
L60
L61
L62
L100
L129
L130
Days after Germination

FIG. 19

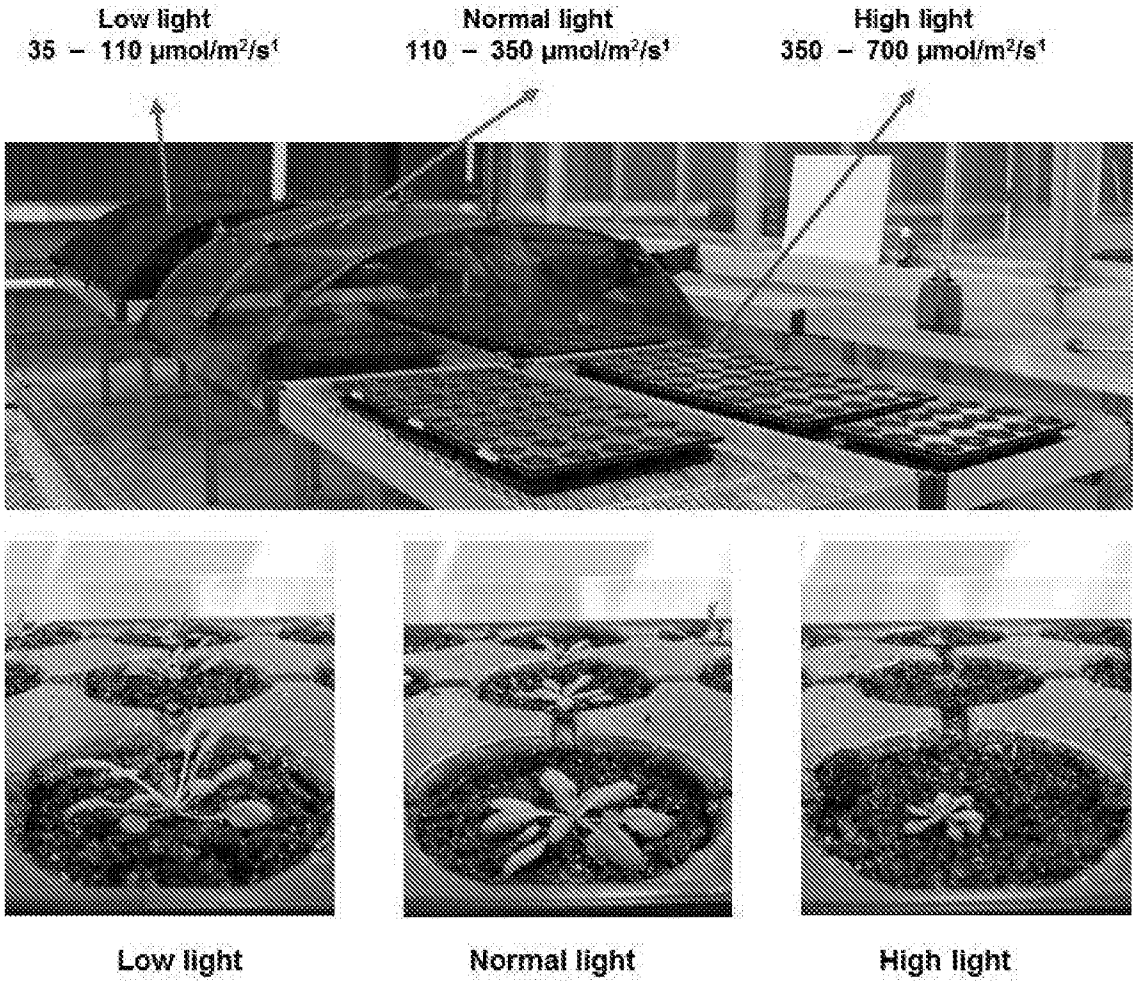

Low light
35 – 110 µmol/m²/s¹
Normal light
110 – 350 µmol/m²/s¹
High light
350 – 700 µmol/m²/s¹
Low light
Normal light
High light

FIG. 20

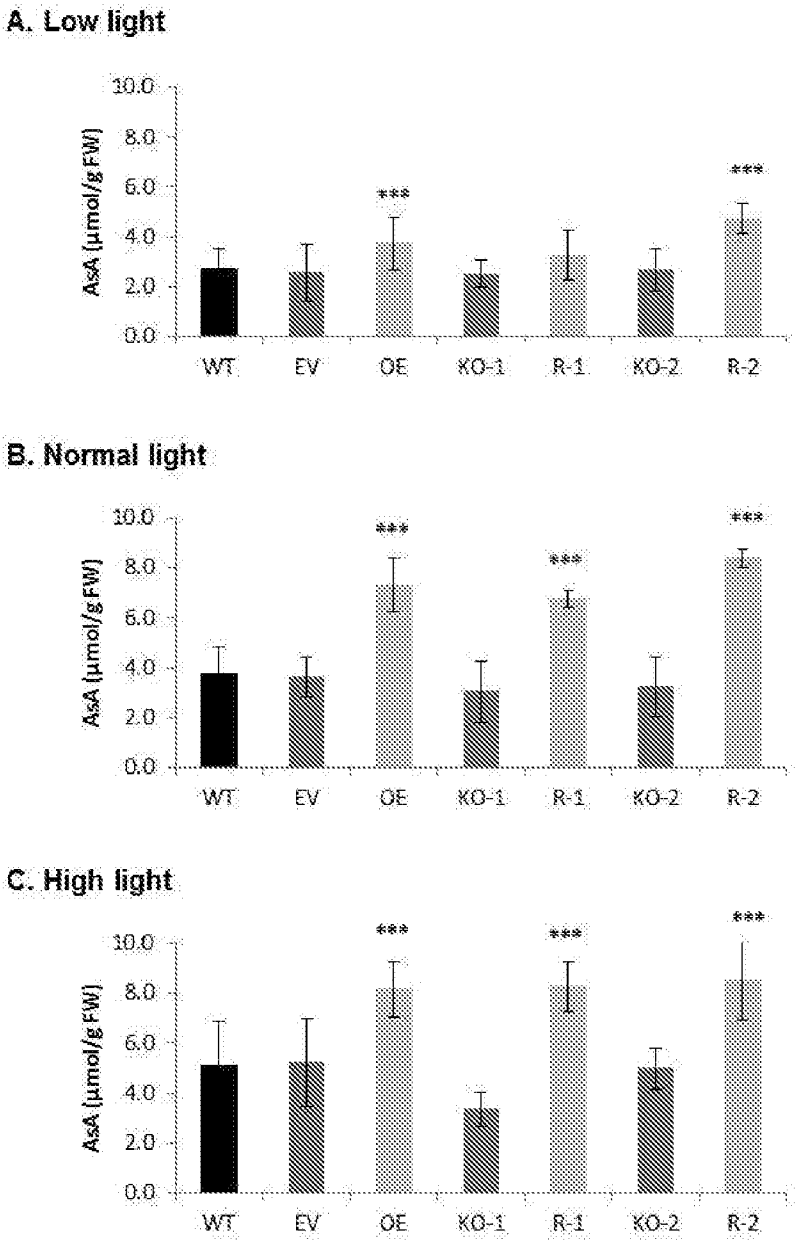

A. Low light
AsA (µmol/g FW)
10.0
8.0
6.0
4.0
2.0
0.0
***
***
WT
EV
OE
KO-1
R-1
KO-2
R-2
B. Normal light
AsA (µmol/g FW)
10.0
8.0
6.0
4.0
2.0
0.0
***
***
***
WT
EV
OE
KO-1
R-1
KO-2
R-2
C. High light
AsA (µmol/g FW)
10.0
8.0
6.0
4.0
2.0
0.0
***
***
***
WT
EV
OE
KO-1
R-1
KO-2
R-2

FIG. 21

Dependent Variable: Expression

Source	DF	Sum of Squares	Mean Square	F Value	Pr > F
Model	20	810.6441505	40.5322075	38.61	<.0001
Error	160	167.9726182	1.0498289		
Corrected Total	180	978.6167688			

R-Square	Coeff Var	Root MSE	Expression Mean
0.782748	21.98923	1.123266	5.108257

Source	DF	Anova SS	Mean Square	F Value	Pr > F
Light	2	349.1287455	174.5643727	166.28	<.0001
Lines	6	418.4714051	69.7452342	66.43	<.0001
Light*Lines	12	43.0440000	3.5870000	3.42	0.0002

FIG. 22

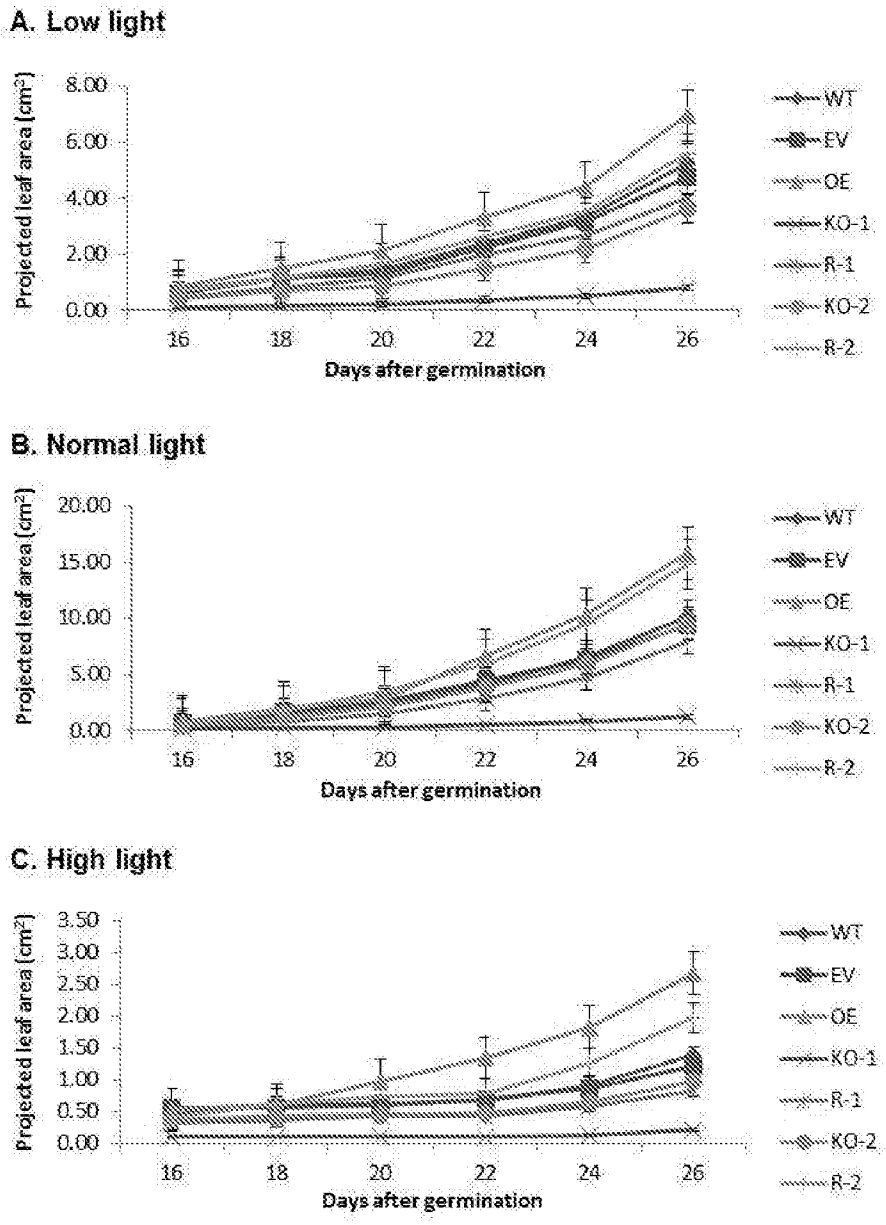

A. Low light
Projected leaf area (cm²)
8.00
6.00
4.00
2.00
0.00
16
18
20
22
24
26
Days after germination
WT
EV
OE
KO-1
R-1
KO-2
R-2
B. Normal light
Projected leaf area (cm²)
20.00
15.00
10.00
5.00
0.00
16
18
20
22
24
26
Days after germination
WT
EV
OE
KO-1
R-1
KO-2
R-2
C. High light
Projected leaf area (cm²)
3.50
3.00
2.50
2.00
1.50
1.00
0.50
0.00
16
18
20
22
24
26
Days after germination
WT
EV
OE
KO-1
R-1
KO-2
R-2

FIG. 23

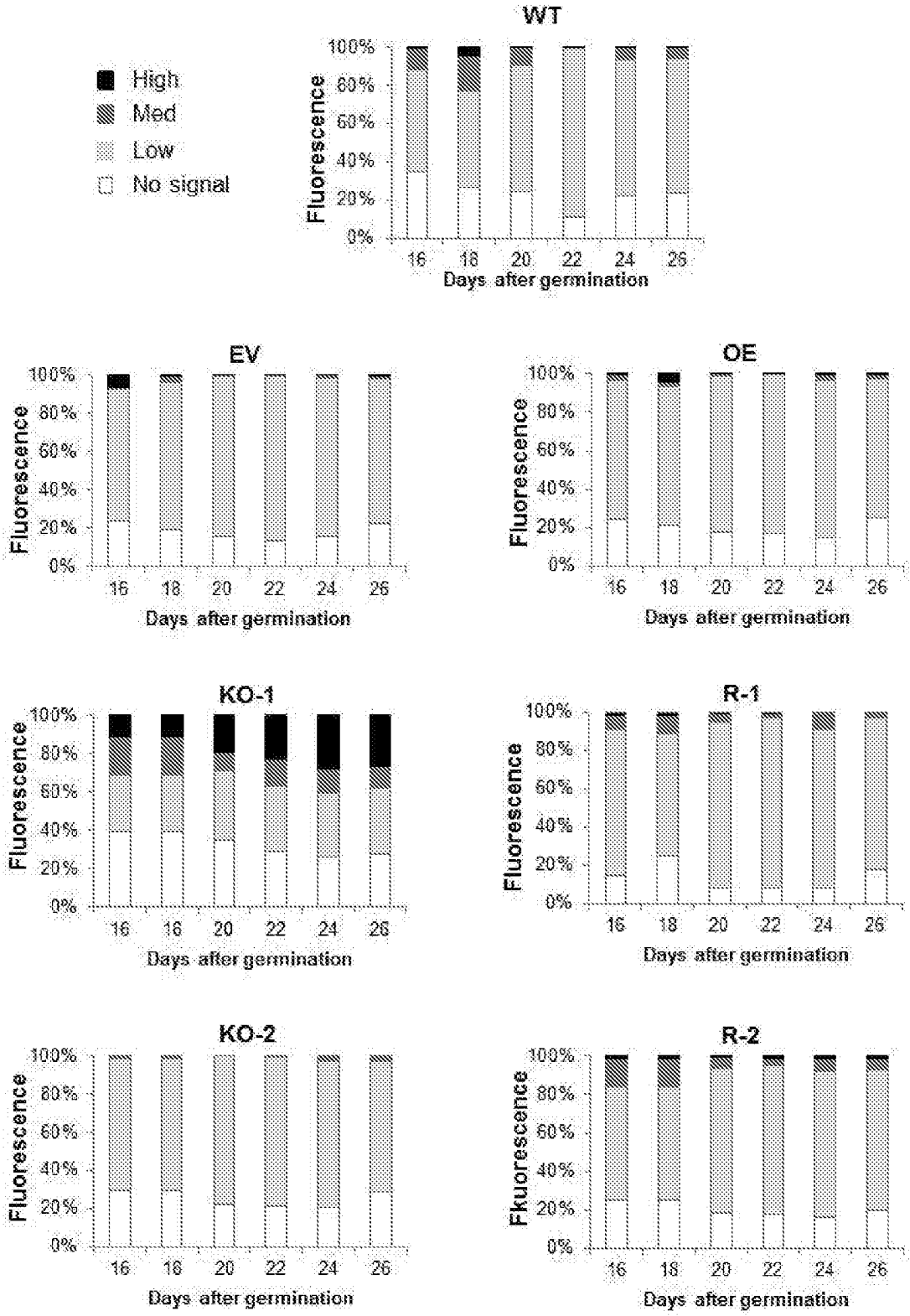

WT
High
Med
Low
No signal
Fluorescence
100%
80%
60%
40%
20%
0%
16
18
20
22
24
26
Days after germination
EV
OE
KO-1
R-1
KO-2
R-2
Fkuorescence

FIG. 24

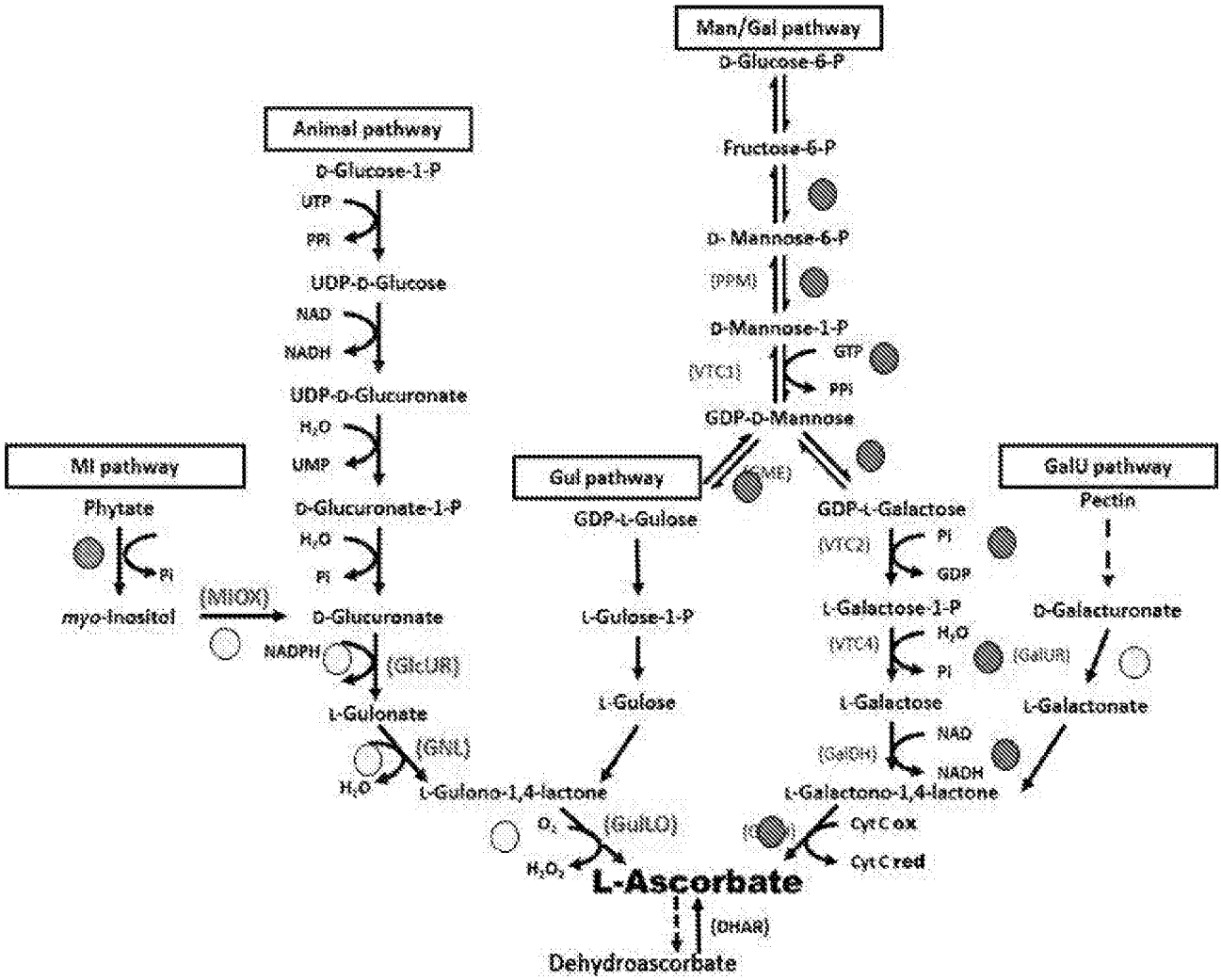

Man/Gal pathway
D-Glucose-6-P
Fructose-6-P
D- Mannose-6-P
(PPM)
D-Mannose-1-P
(VTC1)
GTP
PPi
GDP-D-Mannose
Animal pathway
D-Glucose-1-P
UTP
PPi
UDP-D-Glucose
NAD
NADH
UDP-D-Glucuronate
H2O
UMP
D-Glucuronate-1-P
MI pathway
Phytate
PI
myo-Inositol
(MIOX)
H2O
PI
D-Glucuronate
NADPH
(GlcUR)
L-Gulonate
(GNL)
H2O
Gul pathway
GDP-L-Gulose
(GME)
GDP-L-Galactose
GalU pathway
Pectin
(VTC2)
PI
GDP
L-Galactose-1-P
D-Galacturonate
L-Gulose-1-P
(VTC4)
H2O
PI
(GalUR)
L-Gulose
L-Galactose
L-Galactonate
(GalDH)
NAD
NADH
L-Galactono-1,4-lactone
L-Gulono-1,4-lactone
O2
(GulLO)
H2O2
Cyt C ox
Cyt C red
L-Ascorbate
(DHAR)
Dehydroascorbate

FIG. 25

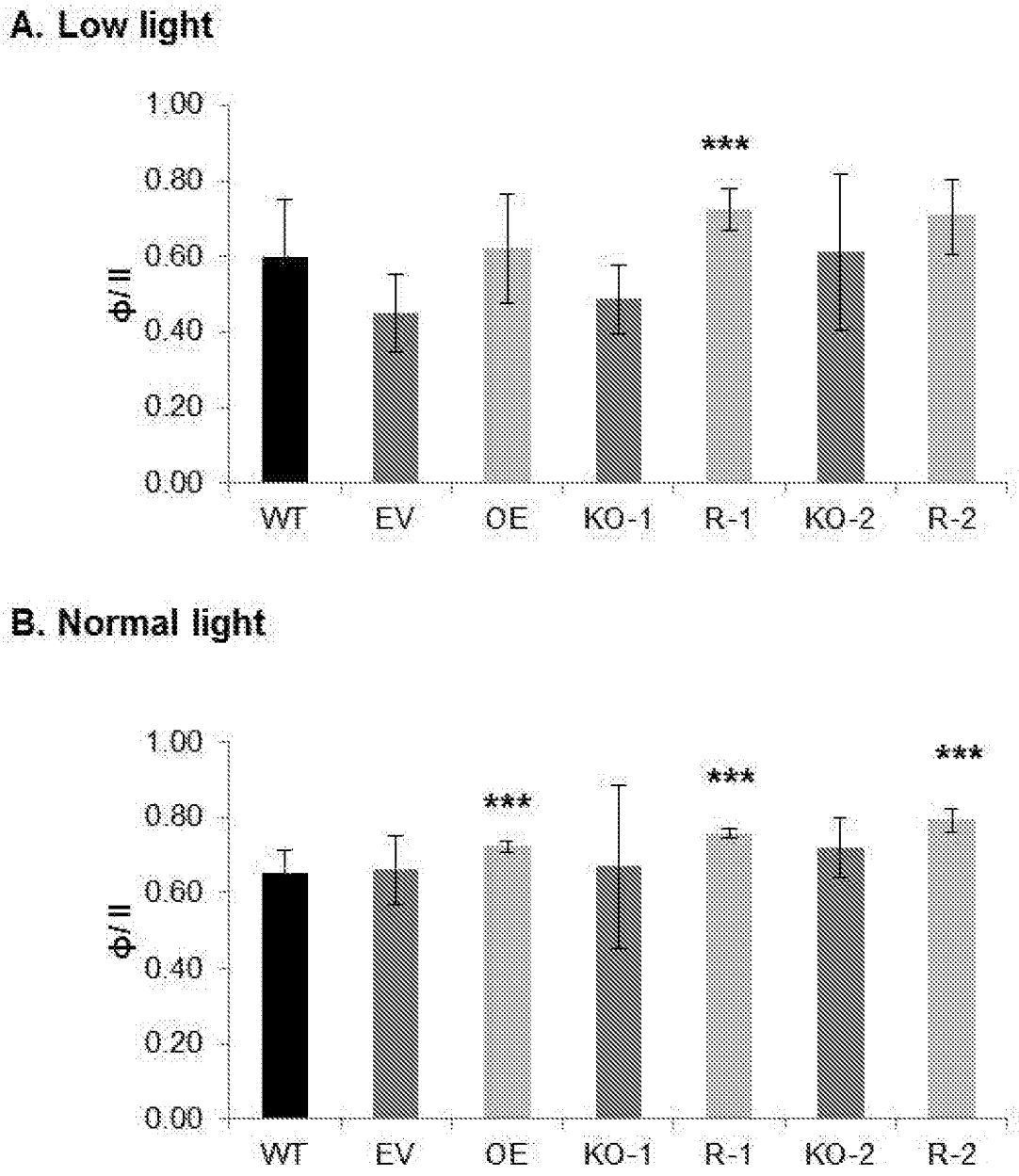

A. Low light
1.00
0.80
0.60
0.40
0.20
0.00
Φ/ II
***
WT
EV
OE
KO-1
R-1
KO-2
R-2
B. Normal light
1.00
0.80
0.60
0.40
0.20
0.00
Φ/ II
***
***
***
WT
EV
OE
KO-1
R-1
KO-2
R-2

FIG. 26

Dependent Variable: Expression

Source	DF	Sum of Squares	Mean Square	F Value	Pr > F
Model	13	1.04174447	0.08013419	6.59	<.0001
Error	112	1.36244350	0.01216467		
Corrected Total	125	2.40418797			

R-Square	Coeff Var	Root MSE	Expression Mean
0.433304	0.433304	0.110294	0.658127

Source	DF	Anova SS	Mean Square	F Value	Pr > F
Light	1	0.58167212	0.09694535	7.97	<.0001
Lines	6	0.34897894	0.34897894	28.69	<.0001
Light*Lines	6	0.11109341	0.01851557	1.52	0.1773

FIG. 27

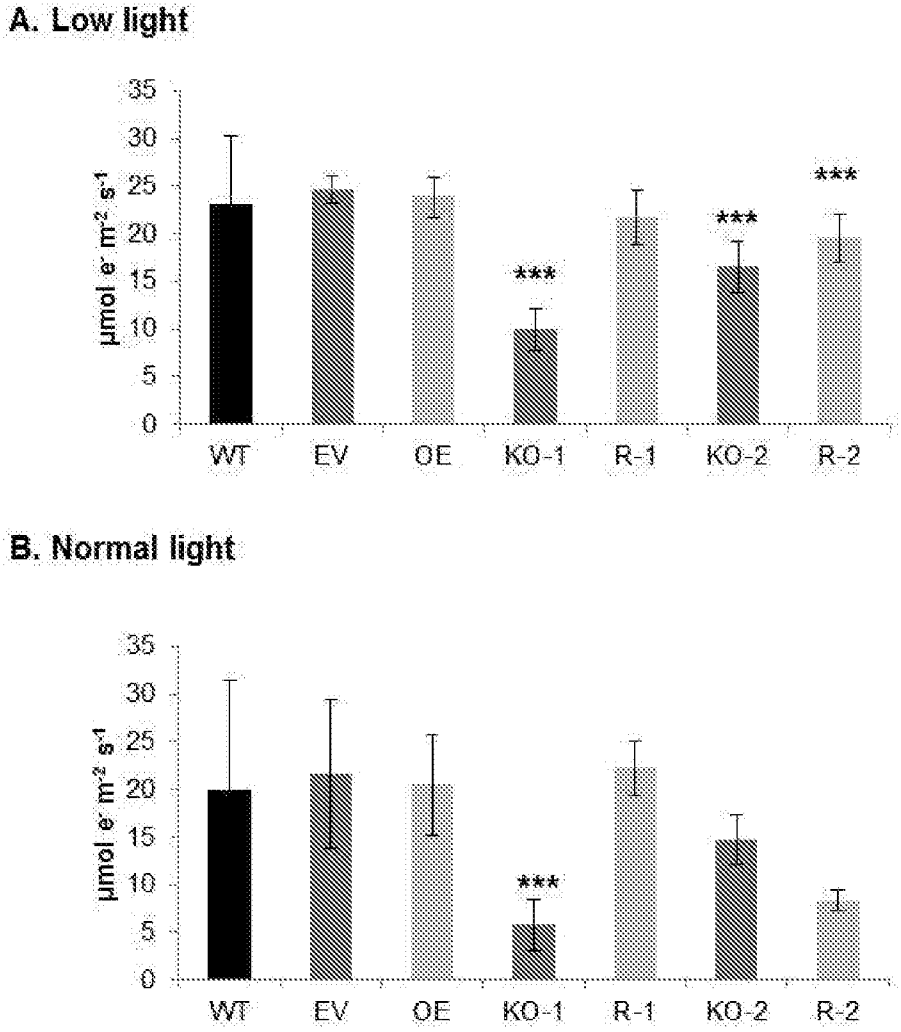

A. Low light
µmol e⁻ m⁻² s⁻¹
35
30
25
20
15
10
5
0
***
***
***
WT
EV
OE
KO-1
R-1
KO-2
R-2
B. Normal light
µmol e⁻ m⁻² s⁻¹
35
30
25
20
15
10
5
0
***
WT
EV
OE
KO-1
R-1
KO-2
R-2

FIG. 28

Dependent Variable: Expression

Source	DF	Sum of Squares	Mean Square	F Value	Pr > F
Model	13	3866.400334	297.415410	11.17	<.0001
Error	112	2982.298147	26.627662		
Corrected Total	125	6848.698481			

R-Square	Coeff Var	Root MSE	Expression Mean
0.564545	27.99361	5.160200	18.43349

Source	DF	Anova SS	Mean Square	F Value	Pr > F
Light	1	332.376931	332.376931	12.48	0.0006
Lines	6	3052.854000	508.809000	19.11	<.0001
Light*Lines	6	481.169403	80.194901	3.01	0.0091

FIG. 29

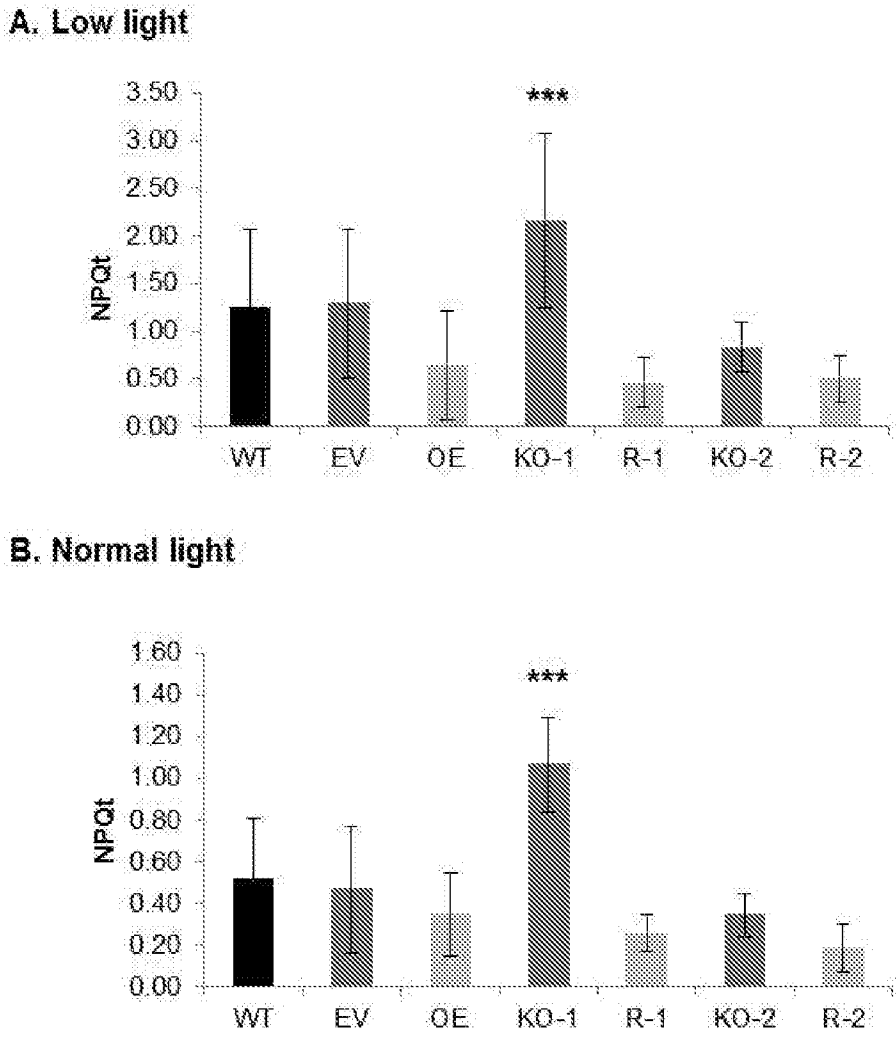

A. Low light
NPQt
3.50
3.00
2.50
2.00
1.50
1.00
0.50
0.00
***
WT
EV
OE
KO-1
R-1
KO-2
R-2
B. Normal light
NPQt
1.60
1.40
1.20
1.00
0.80
0.60
0.40
0.20
0.00
***
WT
EV
OE
KO-1
R-1
KO-2
R-2

FIG. 30

Dependent Variable: Expression

Source	DF	Sum of Squares	Mean Square	F Value	Pr > F
Model	13	28.75697908	2.21207531	6.19	<.0001
Error	112	40.02808137	0.35739358		
Corrected Total	125	68.78506044			

R-Square	Coeff Var	Root MSE	Expression Mean
0.418070	86.62722	0.597824	0.690111

Source	DF	Anova SS	Mean Square	F Value	Pr > F
Light	1	9.43445128	9.43445128	26.40	<.0001
Lines	6	17.23774602	2.87295767	8.04	<.0001
Light*Lines	6	2.08478178	0.34746363	0.97	0.4475

FIG. 31

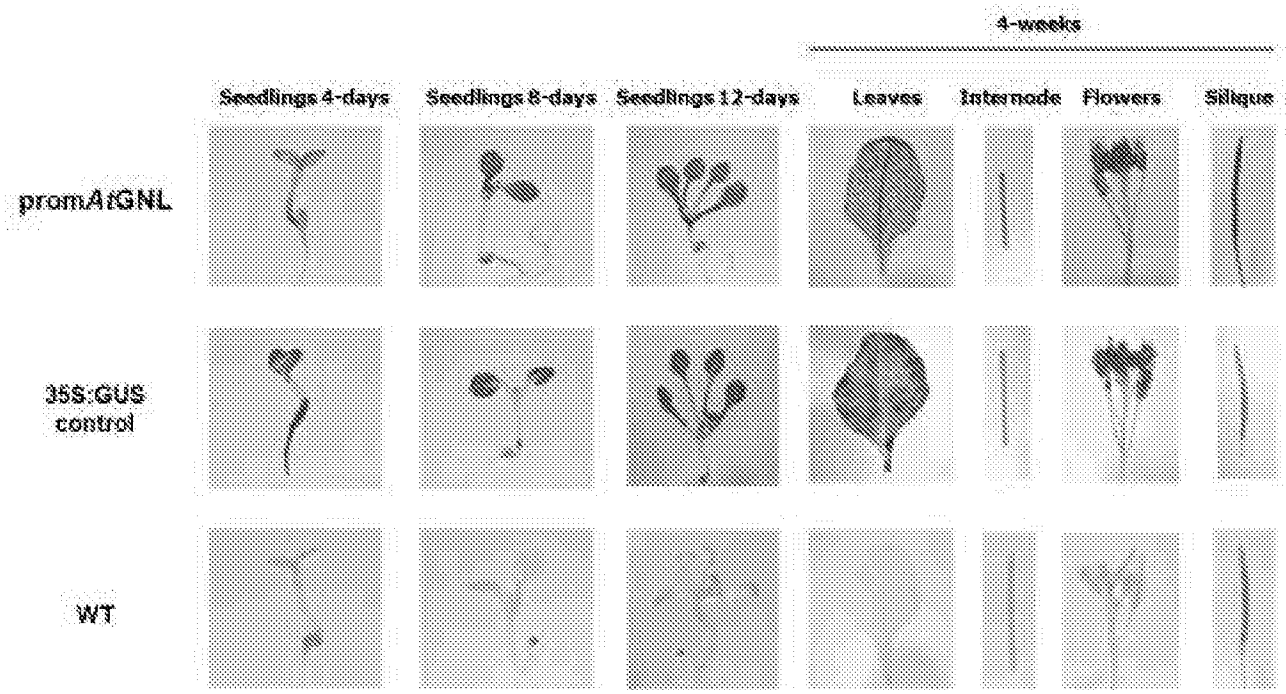

4-weeks
Seedlings 4-days
Seedlings 8-days
Seedlings 12-days
Leaves
Internode
Flowers
Silique
promAtGNL
35S:GUS control
WT

FIG. 32

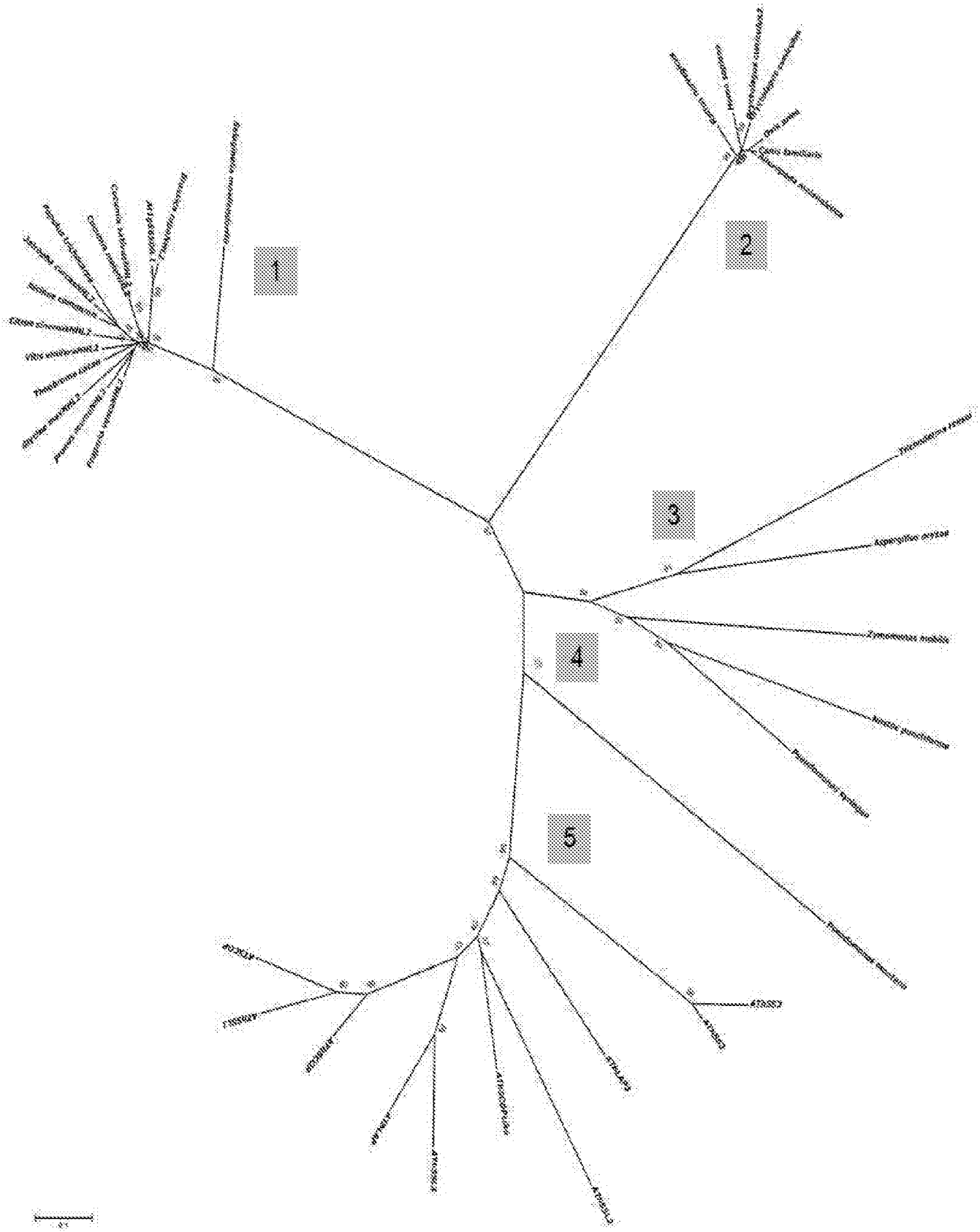


FIG. 33

Species	Description
1. Plants	
*At*1g56500 (*At*GNL)	
Brassica rapa	#Brassica_rapa_:103838684_NHL_repeat-containing_protein_2_(A)
Cucumis sativus	#Cucumis_sativus:101222142_NHL_repeat-containing_protein_2_(A)
Cucumis melo	#Cucumis_melo:103492110_NHL_repeat-containing_protein_2_(A)
Populus trichocarpa	#Populus_trichocarpa_:POPTR_0013s00930g_POPTRDRAFT_1096018_haloacid_dehalogenase-like_hydrolase_family_protein_(A)
Jatropha curcas	#jJatropha_curcas:105647432_NHL_repeat-containing_protein_2_(A)
Ricinus communis	#Ricinus_communis_:RCOM_1435490_2-deoxyglucose-6-phosphate_phosphatase_putative_(EC:5.4.2.6)_(A)
Citrus sinensis	#Citrus_sinensis:102627823_NHL_repeat-containing_protein_2-like_(A)
Vitis vinifera	#Vitis_vinifera:100247769_NHL_repeat-containing_protein_2_(A)
Theobroma cacao	#Theobroma_cacao:TCM_026778_Haloacid_dehalogenase-like_hydrolase_family_protein_(A)
Glycine max	#Glycine_max_:100795843_NHL_repeat-containing_protein_2-like_(A)
Prunus mume	#Prunus_mume:103344235_NHL_repeat-containing_protein_2_(A)
Fragaria vesca	#Fragaria_vesca:101313042_NHL_repeat-containing_protein_2_(A)
Selaginella moellendorffii	#Selaginella_moellendorffii:SELMODRAFT_79954_hypothetical_protein_(A)
2. Animals	
Rattus norvegicus	#Rattus_norvegicus:25106_Rgn_GNL_Rc_Reguc_regucalcin_(senescence_marker_protein-30)_(EC:3.1.1.17)_K01053_gluconolactonase_EC:3.1.1.17_(A)
Homo sapiens	#Homo_sapiens:9104_RGN_GNL_HEL-S-41_RC_SMP30_regucalcin_(EC:3.1.1.17)_K01053_gluconolactonase_EC:3.1.1.17_(A)
Oryctolagus cuniculus 2	#sp|Q9TTJ6|RGN_RABIT_Regucalcin_OSOryctolagus_cuniculus_GNRGN_PE2_SV1

FIG. 34A

Ovis aries	#Ovis_aries_(sheep):100171395_RGN_regucalcin_(senescence_marker_protein-30)_(EC:3.1.1.17)_K01053_gluconolactonase_EC:3.1.1.17_(A)
Canis familliaris	#Canis_familiaris_(dog):480893_RGN_regucalcin_K01053_gluconolactonase_EC:3.1.1.17_(A)
Ailuroposa melanoleuca	#Ailuropoda_melanoleuca_(giant_panda):100467773_RGN_regucalcin_K01053_gluconolactonase_EC:3.1.1.17_(A)
3. Bacteria and fungi	
Trichoderma reesei	#Trichoderma_reesei:TRIREDRAFT_62581_gluconolactonase-like_protein_K01053_gluconolactonase_EC:3.1.1.17_(A)
Aspergillus oryzae	#Aspergillus_oryzae:AOR_1_890114_AO090701000487_protein_AkeP_K01053_gluconolactonase_EC:3.1.1.17_(A)
Zymomonas mobilis	#sp|Q01578|GNL_ZYMMO_Gluconolactonase_OSZymomonas_mobilis_subsp._mobilis_(strain_ATCC_31821_/_ZM4_/_CP4)_GNgnl_PE1_SV2
Nostoc punctiforme	#Nostoc_punctiforme:Npun_F1780_SMP-30/gluconolaconase/LRE_domain-containing_protein_(EC:3.1.1.17)_K01053_gluconolactonase_EC:3.1.1.17_(A)
Pseudomonas syringae	#Pseudomonas_syringae_pv._tomato_DC3000_gluconolactonase_K01053_gluconolactonase_EC:3.1.1.17_(A)
4. Bacteria	
Pseudomonas monteilli	#Pseudomonas_monteilii_SB3101:X970_06765_gluconolactonase_K01053_gluconolactonase_EC:3.1.1.17_(A)
5. *Arabidopsis thaliana*	
AThSS3, AthSS2, AthLAP3, AthSSL2, AThSCOPL, AThSSL3, AThLAP, AThSCOP, AThSSL1, ATSCOP	

FIG. 34B

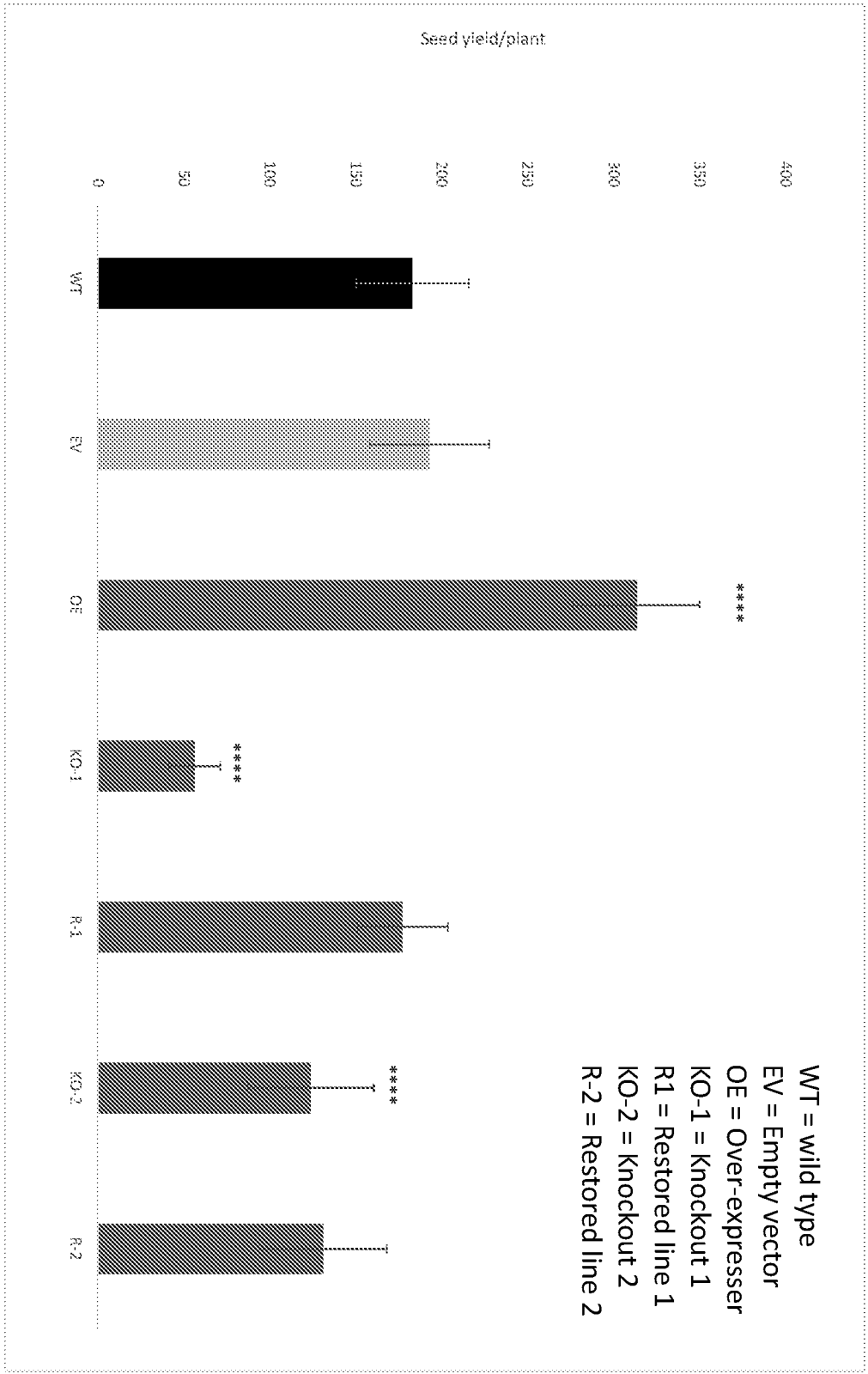

GNL Constitutive Expression Leads to Seed Yield Increase in Arabidopsis
WT = wild type
EV = Empty vector
OE = Over-expresser
KO-1 = Knockout 1
R1 = Restored line 1
KO-2 = Knockout 2
R-2 = Restored line 2
Seed yield/plant
0
50
100
150
200
250
300
350
400
WT
EV
OE
KO-1
R-1
KO-2
R-2
****
****
****
32 biological replicates: were analyzed by ANOVA Tukey's test. ****P<0.0001

FIG. 35

GNL DNA Sequence

```
   1 ATGGCTTTGA AACTCACTTC TCCGCCTTCA GTTTTCTCAC AATCAAGGAG
  51 ATTATCTTCT TCTTCGTTAA TTCCGATAAG GTCAAAATCC ACATTCACCG
 101 GATTTCGATC GAGAACCGGT GTTTATTTAA GCAAAACGAC GGCGCTTCAG
 151 TCGTCTACAA AACTGAGTGT GGCAGCGGAG AGTCCTGCGG CGACAATTGC
 201 GACGGATGAT TGGGGGAAAG TGTCGGCGGT TCTGTTTGAT ATGGACGGTG
 251 TGCTTTGTAA CAGTGAAGAT CTTTCTAGAC GCGCCGCCGT GGATGTTTTT
 301 ACGGAGATGG GAGTTGAAGT CACTGTGGAC GATTTCGTTC CTTTTATGGG
 351 AACAGGTGAA GCCAAGTTTT TAGGAGGTGT TGCTTCAGTC AAAGAAGTTA
 401 AAGGATTTGA TCCAGATGCA GCTAAAGAGA GATTCTTTGA AATATATCTC
 451 GATAAGTATG CGAAGCCAGA ATCTGGGATT GGATTTCCAG GAGCATTGGA
 501 GCTTGTTACT GAGTGTAAGA ACAAAGGCCT TAAAGTCGCT GTTGCATCTA
 551 GTGCTGACCG TATCAAAGTT GATGCGAATC TGAAAGCTGC TGGTTTGTCT
 601 TTGACCATGT TTGATGCCAT TGTTTCAGCA GACGCCTTTG AGAATTTGAA
 651 ACCAGCTCCA GATATTTTCC TGGCTGCTGC AAAGATCTTA GGTGTGCCTA
 701 CCAGCGAGTG TGTTGTTATT GAAGATGCGC TTGCTGGAGT CCAAGCCGCA
 751 CAAGCTGCGA ACATGAGATG TATAGCCGTA AAAACTACTT TATCTGAAGC
 801 AATTCTTAAG GATGCTGGTC CTTCTATGAT ACGAGACGAT ATTGGAAACA
 851 TCTCAATCAA TGACATTCTC ACTGGTGGCT CAGATTCTAC CAGAAATTCC
 901 ACAGCAATGC TTGAAGAGAA CACGGTCAGC GACAAAACCA GCGCTAACGG
 951 GTTTCAGGGC TCTCGACGAG ATATACTGAG GTATGGGAGT CTTGGCATTG
1001 CTCTTTCTTG TGTCTACTTC GCCGCCACCA ACTGGAAGGC AATGCAATAT
1051 GCTTCTCCGA AAGCTTTGTG GAATGCATTG GTTGGAGCAA AAAGCCCTTC
1101 TTTTACACAG AACCAAGGTG AAGGGAGAGT GCAACAGTTC GTCGATTACA
1151 TTGCTGATCT AGAGAGCAAG CAAACAGCTA CAACTGTGCC AGAATTCCCA
1201 TCTAAACTCG ACTGGCTAAA CACTGCCCCT CTCCAGTTTC GCCGGGATTT
1251 AAAAGGGAAA GTGGTTATAC TTGATTTTTG GACCTATTGC TGCATAAACT
1301 GTATGCATGT ATTACCGGAT CTAGAGTTTC TTGAGAAGAA GTACAAGGAT
```

FIG. 36A

1351 ATGCCATTCA CCGTTGTGGG TGTACACTCG GCTAAGTTCG ACAATGAGAA

1401 AGATTTAGAT GCCATACGAA ATGCAGTTCT TCGCTATGAT ATTAGCCACC

1451 CGGTTGTGAA TGATGGAGAC ATGTACATGT GGAGAGAGCT TGGCATCAAC

1501 TCGTGGCCTA CATTTGCTGT TGTTTCTCCT AATGGCAAAG TCATTGCACA

1551 AATTGCCGGA GAAGGTCACC GCAAAGATCT TGATGACGTG GTGGCGGCAG

1601 CTCTGACATA TTATGGTGGA AAGAATGTAT TAGACAGTAC TCCGCTTCCA

1651 ACACGTTTGG AGAAAGACAA CGATCCACGT TTGGCCACGT CTCCGTTGAA

1701 ATTTCCGGGA AAGTTGGCTA TTGATACTCT TAATAACAGG CTATTCATCT

1751 CAGACAGTAA CCATAACCGT ATTATTGTAA CTGATCTCGA AGGAAATTTC

1801 ATAGTCCAAA TTGGCAGCAG TGGAGAAGAA GGTTTCCAAG ATGGTTCCTT

1851 CGAAGATGCT GCATTTAATC GTCCTCAGGG ACTAGCTTAT AATGCTAAGA

1901 AGAATCTTCT TTATGTTGCT GACACCGAGA ATCATGCTTT GAGAGAGATT

1951 GATTTTGTCA ACGAGAGAGT ACAGACTCTG GCTGGTAATG GAACTAAAGG

2001 CTCAGACTAC CAAGGTGGAA GAAAAGGAAC CAAACAGCTT TTGAATTCTC

2051 CTTGGGACGT ATGCTTTGAG CCGGTGAATG AGAAGGTATA CATTGCAATG

2101 GCAGGTCAGC ACCAGATTTG GGAATACAGT GTGCTTGATG GTATTACTCG

2151 AGTTTTCAGT GGAAATGGTT ATGAAAGAAA CCTCAACGGT TCCACCCCTC

2201 AGACTACATC ATTTGCTCAG CCATCAGGAA TCTCATTAGG CCCTGATTTG

2251 AAAGAAGCAT ATATTGCTGA TAGCGAGAGC AGTTCTATTC GTGCCCTTGA

2301 TCTTCAAACT GGAGGATCAA GATTACTTGC GGGTGGTGAT CCGTATTTCT

2351 CTGAGAATCT TTTCAAGTTT GGAGACAATG ATGGCGTGGG AGCAGAAGTT

2401 CTCCTACAAC ACCCGCTAGG TGTATTATGC GCAAATGATG GTCAAATATA

2451 TCTAACTGAT AGCTATAACC ACAAGATTAA GAAGTTGGAC CCTGTAACCA

2501 AACGTGTTGT TACTCTCGCT GGAACGGGAA AAGCCGGTTT TAAGGATGGG

2551 AAGGTCAAGG GTGCTCAGCT TTCAGAGCCT GCAGGACTTG CTATAACTGA

2601 AAACGGGAGG CTGTTTGTGG CGGATACAAA TAATAGCCTT ATCCGATACA

2651 TAGATTTGAA CAAAGGAGAA GACTCAGAGA TTCTTACATT GGAGTTAAAA

2701 GGTGTTCAAC CACCAACGCC AAAGGCAAAA TCCCTGAAAC GTTTGAGAAA

2751 ACGTGCCTCG GCTGATACAA AGATTGTCAA AGTGGATTCT GTAACGTCCC

2801 GTGAAGGAGA TTTGAATCTC AAAATCTCAT TACCAGATGG CTACCATTTC

2851 TCCAAGGAAG CGCGGAGTAA GTTTGTGGTT GATGTGGAGC CTGAAAACGC

FIG. 36B

2901 AGTAGCAATC GATCCAACGG AAGGAACTCT GAGTCCCGAA GGTTCAACAA

2951 TGCTTCATTT TATACAATCT TCAACTTCGG CTTCTGTTGG GAAAATCAGT

3001 TGCAAGGTGT ACTATTGCAA AGAAGACGAG GTTTGCTTGT ATCAGTCTGT

3051 ACAGTTTGAG GTCCCTTTCA AGGTGGAATC AGAATTATCT GCTTCTCCGA

3101 CAATCACATT CACGGTTACA CCGAGAGCAC CCGATGCTGG TGGGTTACAG

3151 CTTCAAGGTA CTCGCTGA

FIG. 36C

GNL Amino Acid Sequence

```
   1 MALKLTSPPS VFSQSRRLSS SSLIPIRSKS TFTGFRSRTG VYLSKTTALQ
  51 SSTKLSVAAE SPAATIATDD WGKVSAVLFD MDGVLCNSED LSRRAAVDVF
 101 TEMGVEVTVD DFVPFMGTGE AKFLGGVASV KEVKGFDPDA AKERFFEIYL
 151 DKYAKPESGI GFPGALELVT ECKNKGLKVA VASSADRIKV DANLKAAGLS
 201 LTMFDAIVSA DAFENLKPAP DIFLAAAKIL GVPTSECVVI EDALAGVQAA
 251 QAANMRCIAV KTTLSEAILK DAGPSMIRDD IGNISINDIL TGGSDSTRNS
 301 TAMLEENTVS DKTSANGFQG SRRDILRYGS LGIALSCVYF AATNWKAMQY
 351 ASPKALWNAL VGAKSPSFTQ NQGEGRVQQF VDYIADLESK QTATTVPEFP
 401 SKLDWLNTAP LQFRRDLKGK VVILDFWTYC CINCMHVLPD LEFLEKKYKD
 451 MPFTVVGVHS AKFDNEKDLD AIRNAVLRYD ISHPVVNDGD MYMWRELGIN
 501 SWPTFAVVSP NGKVIAQIAG EGHRKDLDDV VAAALTYYGG KNVLDSTPLP
 551 TRLEKDNDPR LATSPLKFPG KLAIDTLNNR LFISDSNHNR IIVTDLEGNF
 601 IVQIGSSGEE GFQDGSFEDA AFNRPQGLAY NAKKNLLYVA DTENHALREI
 651 DFVNERVQTL AGNGTKGSDY QGGRKGTKQL LNSPWDVCFE PVNEKVYIAM
 701 AGQHQIWEYS VLDGITRVFS GNGYERNLNG STPQTTSFAQ PSGISLGPDL
 751 KEAYIADSES SSIRALDLQT GGSRLLAGGD PYFSENLFKF GDNDGVGAEV
 801 LLQHPLGVLC ANDGQIYLTD SYNHKIKKLD PVTKRVVTLA GTGKAGFKDG
 851 KVKGAQLSEP AGLAITENGR LFVADTNNSL IRYIDLNKGE DSEILTLELK
 901 GVQPPTPKAK SLKRLRKRAS ADTKIVKVDS VTSREGDLNL KISLPDGYHF
 951 SKEARSKFVV DVEPENAVAI DPTEGTLSPE GSTMLHFIQS STSASVGKIS
1001 CKVYYCKEDE VCLYQSVQFE VPFKVESELS ASPTITFTVT PRAPDAGGLQ
1051 LQGTR
```

FIG. 37

INTERNATIONAL SEARCH REPORT

International application No.
PCT/US17/64286

A. CLASSIFICATION OF SUBJECT MATTER

IPC - A01H 5/00; C12N 1/13, 5/10, 9/90, 15/09, 15/82 (2018.01)
CPC - A01H 5/00; C12N 5/10, 9/90, 15/09, 15/82, 15/8243; C12P 17/04

According to International Patent Classification (IPC) or to both national classification and IPC

B. FIELDS SEARCHED

Minimum documentation searched (classification system followed by classification symbols)
See Search History document

Documentation searched other than minimum documentation to the extent that such documents are included in the fields searched
See Search History document

Electronic data base consulted during the international search (name of data base and, where practicable, search terms used)
See Search History document

C. DOCUMENTS CONSIDERED TO BE RELEVANT

Category*	Citation of document, with indication, where appropriate, of the relevant passages	Relevant to claim No.
A	US 2002/0012979 A1 (BERRY et al.) January 31, 2002; abstract; paragraphs [0036], [0040]; claim 60	1-20
A	EP 1026257 A1 (F. HOFFMANN-LA ROCHE AG) August 9, 2000; claim 1	1-20
A	US 2011/244512 A1 (HONG et al.) October 6, 2011; abstract; paragraph [0122]; claims 1, 4	1-20
A	WO 2011/050286 A1 (ARKANSAS STATE UNIVERSITY) April 28, 2011; figure 1; claims 1, 12, 32	1-20

☐ Further documents are listed in the continuation of Box C. ☐ See patent family annex.

* Special categories of cited documents:
"A" document defining the general state of the art which is not considered to be of particular relevance
"E" earlier application or patent but published on or after the international filing date
"L" document which may throw doubts on priority claim(s) or which is cited to establish the publication date of another citation or other special reason (as specified)
"O" document referring to an oral disclosure, use, exhibition or other means
"P" document published prior to the international filing date but later than the priority date claimed
"T" later document published after the international filing date or priority date and not in conflict with the application but cited to understand the principle or theory underlying the invention
"X" document of particular relevance; the claimed invention cannot be considered novel or cannot be considered to involve an inventive step when the document is taken alone
"Y" document of particular relevance; the claimed invention cannot be considered to involve an inventive step when the document is combined with one or more other such documents, such combination being obvious to a person skilled in the art
"&" document member of the same patent family

Date of the actual completion of the international search	Date of mailing of the international search report
05 February 2018 (05.02.2018)	22 FEB 2018
Name and mailing address of the ISA/ Mail Stop PCT, Attn: ISA/US, Commissioner for Patents P.O. Box 1450, Alexandria, Virginia 22313-1450 Facsimile No. 571-273-8300	Authorized officer Shane Thomas PCT Helpdesk: 571-272-4300 PCT OSP: 571-272-7774

Form PCT/ISA/210 (second sheet) (January 2015)